FACULTY OF TECHNOLOGY AND
MARITIME SCIENCES

Local Synthesis and Direct Integration of Carbon Nanotubes into Microsystems for Sensor Applications

Doctoral Thesis

Bao Quoc Ta

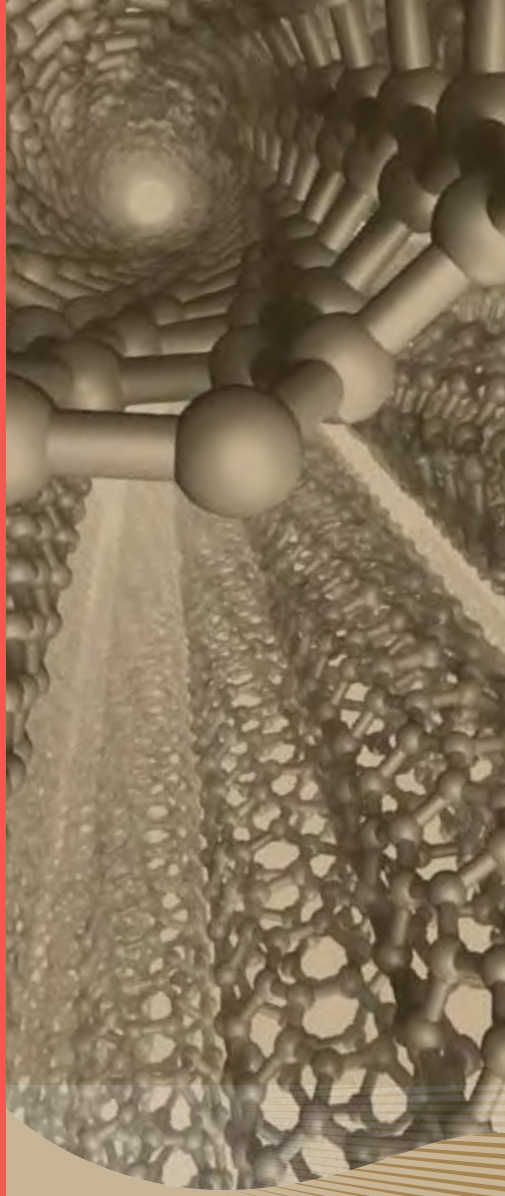

2014

FACULTY OF TECHNOLOGY AND MARITIME SCIENCES

Local Synthesis and Direct Integration of Carbon Nanotubes into Microsystems for Sensor Applications

Thesis submitted for the degree of Philosophiae Doctor

Bao Quoc Ta

Department of Micro- and Nanosystem Technology (IMST)
Faculty of Technology and Maritime Sciences (TekMar)
Buskerud and Vestfold University College (HBV)
Horten, 2014

Local Synthesis and Direct Integration of Carbon Nanotubes into Microsystems for Sensor Applications

Department of Micro- and Nanosystem Technology (IMST)
Faculty of Technology and Maritime Sciences (TekMar)
Buskerud and Vestfold University College (HBV)
Horten, 2014

Doctoral theses at Buskerud and Vestfold University College, no. 1

ISSN: 1894-6380 (print)
ISSN: 1894-7530 (online)
ISBN: 978-82-7860-241-6 (print)
ISBN: 978-82-7860-242-3 (online)

Cover: HBV, Kommunikasjonsseksjonen
Printed at LOS digital

Abstract

Carbon nanotubes (CNTs) have been intensively studied since their discovery more than two decades ago. A lot of research has exploited their extraordinary properties and various applications, meanwhile, revealed the challenges of fabricating the CNT-based device. Major challenges concern the high temperature required for the CNT growth, and the difficulty in handling and maneuvering the CNTs. An innovative approach to overcome these challenges is to locally synthesize and directly assemble CNTs into devices. Following such approach, this thesis developed a fabrication process with a high simplicity, a high controllability, and a CMOS/MEMS compatibility for the local synthesis and direct integration of CNTs into Si microsystems. This thesis covers the total process chain: from synthesis and integration of CNTs, to characterization, and to testing of a proof-of-principle gas sensor.

The first key finding of this thesis is a simple and robust method to control the temperature for the growth of CNTs by using only electrical signals. During the growth process, a localized hot region for the growth of CNTs is created by locally heating a Si microelectrode (Joule heating). The induced temperature is monitored through *in-situ* measurements of the electrical resistance of the Si electrode. The measured resistance provides feedback to control the input power for heating the Si electrode. This pure electrical control enables a simple, automated and parallel process to synthesize locally and integrate CNTs directly into microsystems.

The second key finding of this thesis is the diameter dependency for the effect of an applied electric field on the growth orientation of CNTs. A statistical analysis of 1100 CNTs showed that small-diameter CNTs ($d < 5$ nm) were straight and well-aligned with the applied electric field, whereas the large-diameter CNTs ($d > 10$ nm) were curved and did not align. In the transition regime, CNTs were moderately curved, but the average direction was at small angle with the electric field direction.

The third key finding of this thesis is the correlation between local temperature and resulting characteristics of CNTs. A high gradient of temperature along the Si microelectrode due to Joule heating allowed for studying the effect of temperature. At the region where the temperature is highest ($\sim$900^{o}C), the nanostructure of CNTs had the highest degree of order, and the average diameter of CNT was smallest. At regions with lower temperatures, CNTs had a higher degree of defects and disorder, and a lower average diameter. The density of CNTs, however, was highest at the moderate-temperature region ($\sim$850^{o}C).

The other contribution of this thesis is preliminary results on the development of CNT-based microsystems towards sensor applications. The preliminary results suggest that: (i) contact resistance at the CNT-Si interface could be reduced by both techniques of local annealing and local deposition of Platinum onto the CNT-Si contacts; (ii) thermal evaporation of metals could be used to functionalize the CNTs in a microsystem where CNTs are suspended and span two microelectrodes.

Key words: Carbon nanotubes, Local synthesis, Direct integration, Nanoscale assembly, Gas sensors, Electric-field-assist growth.

Preface

This thesis is submitted in partial fulfillment of the requirements for the degree of Philosophiae Doctor from the Department of Micro- and Nanosystem Technology (IMST), at Buskerud and Vestfold University College (HBV).

This doctoral work has been conducted from September 2010 to December 2013, with Professor Knut E. Aasmundtveit as main supervisor and with co-supervisors Professor Nils Hoivik and Professor Einar Halvorsen.

Financial support was provided by the KD program (08669) at IMST-HBV. Additional supports were given by the Norwegian Micro- and Nano- Fabrication Facility, NorFab (197411, V30), and the Norwegian PhD Network on Nanotechnology for Microsystems, NanoNetwork (190086, S10).

Acknowledgements

I would like to express my special appreciation and gratitude to my supervisors, Professor Knut E. Aasmundtveit, Professor Nils Hoivik, and Professor Einar Halvorsen, for their valuable guidance and advices. Their advices have been very helpful to both my academic and personal developments. *Be clear, Be precise, Be consistent, Be professional* are among their advices that will surely come along with me for the rest of my life. I have been very impressed on how wise, precise, clear, consistent and professional they are. I have set a goal for 10 years to come, that, people will admire me as much as I admire my supervisors now. I would like to give a special thanks to Professor Knut E. Aasmundtveit for seeing my personal strengths and weaknesses and lifting me when I was down. He did not have to care, but he cared, and I am thankful to him for that.

I would like to give sincere thanks to Ragnar D. Johansen, Thomas Martinsen, Zekija Ramic and other lab engineers for their supports for my experimental work. I would also like to thank Ida Noddeland for training and supporting me to use the characterization instruments at the NanoLab NTNU.

I would like to thank the Department of Micro- and Nanosystem Technology, at Buskerud and Vestfold University College, for offering me this PhD position. My sincere thanks also go to the Norwegian Micro–and Nano–Fabrication Facility, NorFab, and the Norwegian PhD Network on Nanotechnology for Microsystems, NanoNetwork for the financial supports.

I would also like to thank Professor Liwei Lin and Dr. Heather Chiamori for the collaboration. Besides academic achievements, I also got great experience during the time I worked with them, at the University of California, Berkeley. Five months being there is a great memory for my life.

I would also like to thank Huy Q. Nguyen, Tormod B. Haugen, Anh V. Ngo, and Thy A. T. Nguyen for taking part in the CNT research group with me. I was very happy to be their co-supervisor and collaborator.

I would like to thank many friends of mine for encouraging me during my doctoral work. Special thanks go to Cuong Phu Le, Maija Heinila, Sanda Knutson, Jani Christoffer Vik, Kjell Hagen and Hege Hagen.

Last but not least, I am thankful to my family and my close friends in Vietnam. They are the biggest motivators and supporters for me to go this far in my academic journey.

Contents

Chapter 1

Research Motivations and Contributions

1.1 Research context and motivations

Carbon nanotubes (CNTs) have been of great interest since their discovery by Iijima [1] more than two decades ago. CNTs are allotropes of carbon with a cylindrical nanostructure. A CNT can be conceptualized by wrapping one or several graphene sheets into a seamless cylinder, as illustrated in Figure 1.1. CNTs are commonly classified into two types: single-walled CNTs or multi-walled CNTs. A single-walled nanotube (SWNT) consists of a single graphene sheet. A multi-walled nanotube (MWNT) consists of more than one graphene sheet. SWNTs have a typical diameter of 1.0-1.5 nm [2]. MWNTs have typical diameters ranging from 5 nm to hundreds of nanometers [3]. CNTs are also classified by their chirality. The chirality of a CNT can be expressed as a pair of indices (n,m) that indicates the direction of wrapping the graphene sheet to form the CNT (as depicted in Figure 1.1). If m = n, the CNT structure is called "armchair" and the CNT exhibits metallic behavior. Otherwise, the CNT exhibits semiconducting behavior with a bandgap ranging from very small to moderate, depending on the indices (m,n). CNTs have a very high aspect ratio: their length can be 10^8 times greater than their diameter [4].

CNTs have become a *de facto* symbol of nanotechnology for their extraordinary properties and applications in various fields. Some of their extraordinary properties are

(i) *Young's modulus* on the order of 1000 GPa (experimental measurement [5, 6] and molecular dynamics simulation [7]). Tensile strength can be up to 150 GPa (experimental measurement [6], and molecular dynamics simulation [8]). Diamond has a comparable strength with CNT, but it is about three times heavier than CNT.

(ii) *Thermal conductivity* can be greater than 3000 $Wm^{-1}K^{-1}$ at room temperature [9] (compared with 2000–2500 $Wm^{-1}K^{-1}$ for diamond [10]).

(iii) *Current density* can be higher than $10^9 Acm^{-2}$ [11]. CNTs can exhibit ballistic transport at room temperature [12].

(iv) *Surface-to-volume ratio* is extremely high. This property is ideal for sensor applications [13, 14].

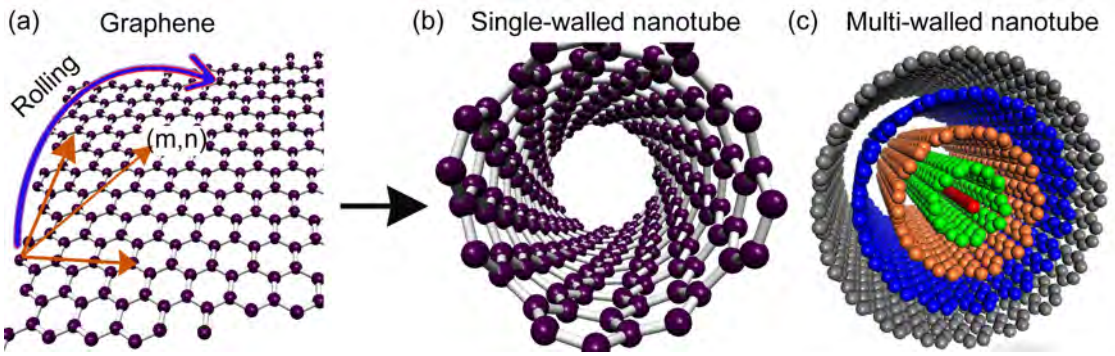

Figure 1.1: Sketch of the CNT structure. A single-walled (or multi-walled) CNT is conceptually formed by wrapping a single sheet (or multiple sheets) of graphene. (a) A graphene sheet: a monolayer of carbon atoms packed into a dense honeycomb crystal structure. (b) A single-walled CNT. (c) A multi-walled CNT.

The properties of CNTs are being exploited in nano-electronic devices, gas/chemicals/bio sensors and more [15–18] . Researchers have shown the extraordinary properties and applications of CNTs, and at the same time revealed the challenges of fabricating the CNT-based devices. Major challenges concern the high temperature required for CNT synthesis and the difficulty in handling and positioning CNTs into micro- and nano-systems.

A solution to these challenges is to localize the synthesis of CNTs and directly assemble the CNTs into the devices. This approach is referred to as Local Synthesis and Direct Integration of CNTs. Details about this approach will be presented in Chapter 2, section 2.4. Following such an approach, this thesis aims to develop a well-controlled, single-step, automated, wafer-level and CMOS/MEMS-compatible process for the synthesis and integration of CNTs into Si microsystems.

There are various methods for the synthesis of CNTs. Most methods are not well-suited for the local synthesis and direct integration. A comparison of typical synthesis methods is presented in Figure 1.2. Criteria for the comparison are: the controllability of the diameter, the density, and the growth orientation of CNTs; as well as the possibility for direct integration of CNTs into microsystems. Three main methods for CNT synthesis are Arc Discharge [1, 19–22], Laser Ablation [23–28] and Chemical Vapor Deposition (CVD) [29–31]. Details about these methods will be presented in Chapter 2. Arc discharge and Laser Ablation methods require a very high temperature for the growth of CNTs (>1000^{o}C), and have a low controllability of the characteristics and the location of CNTs. Accordingly, these methods are not well-suited for the direct synthesis and integration of CNTs into microsystems. Regarding CVD method, there are a variety of modified techniques. Common CVD techniques still require the entire synthesis chamber to be at a high temperature (>600^{o}C), but have a better controllability than Laser Ablation and Arc Discharge. These techniques are commonly used for bulk synthesis of CNTs. Additional processes are thus required for handling, maneuvering and assembling individual CNTs into microsystems after the synthesis of CNTs. Such processes are normally complicated and expensive. In advanced CVD techniques, these processes are no longer required, since CNTs are synthesized at a pre-specified location, and are directly assembled into microsystems. Such advanced CVD techniques

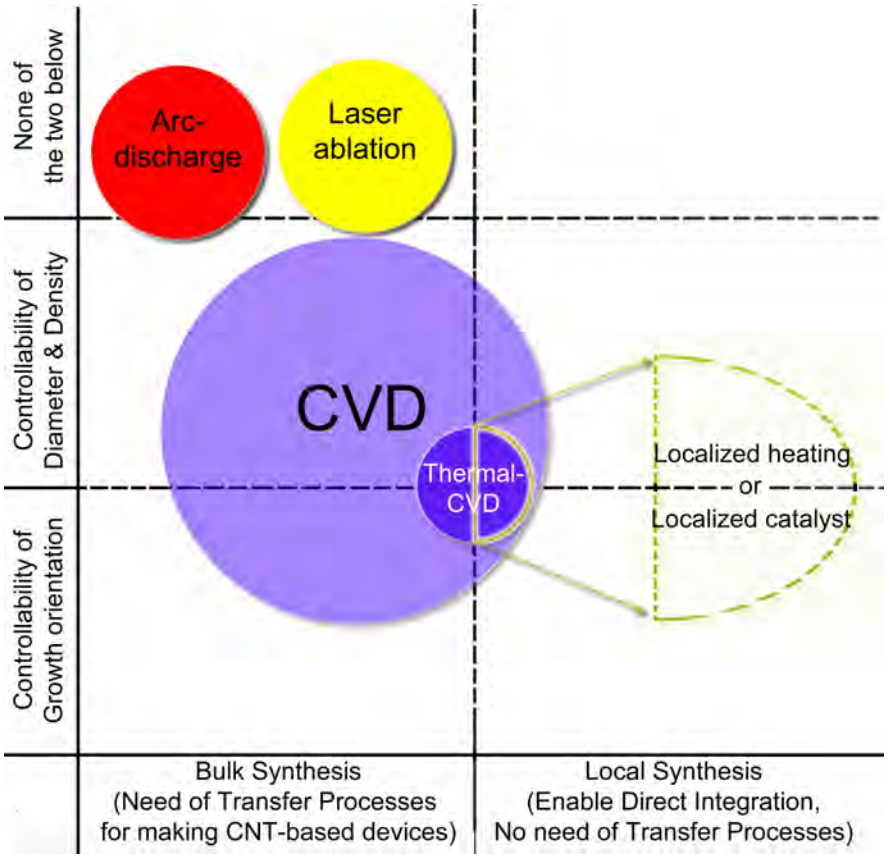

Figure 1.2: A comparison of the CNT synthesis methods, based on the following criteria: controllability of diameter, density and growth orientation of CNTs, as well as the possibility for the direct integration of CNTs into microsystems.

are referred to as "localized CVD synthesis". These techniques enable the localized growth of CNTs by either localizing the position of catalyst, or localizing the thermal environment for the growth of CNTs, or both. The former approach (referred to as "localized catalyst") can only solve the problem of direct assembly of CNTs. The latter approach (referred to as "localized heating") can solve both the problems of high temperature and the direct assembly.

A lot of research on the localized CVD synthesis has been reported. Addressing the "localized catalyst" approach, Jungen *et al.* demonstrated a process using photolithography and lift-off to localize the catalyst locations on a polysilicon microsystem [32–34]. By means of a common CVD process, the authors then obtained a CNT-based device where the CNTs located only at pre-specified locations. A similar technique was also implemented by Dong *et al.*. Addressing the "localized heating" approach, Englander *et al.* [35, 36], Christensen *et al.* [37] and Kawano *et al.* [38] used the resistive heating of Si microheaters to provide a localized hot region for the growth of CNTs, while keeping the surroundings at room temperature. This approach has also been applied by Engstrom *et al.* [39] and Kim *et al.* [40]. Zhou *et al.* [41] also used microheaters, but made of polysilicon instead of single crystalline silicon. Being more differentiating, Dittmer *et al.* [42–44], Zhou *et al.* [45] and Lin *et al.* [46] used metal microheaters, instead of silicon microheaters.

The "localized heating" approach is, however, not limited to the resistive heating technique. The utilization of laser-assisted [47–50], plasmon-assisted [51,52], or inductive heating techniques [53] has also been demonstrated.

This thesis follows the approach of "localized heating". Both polysilicon and single-crystalline silicon microheaters were used. Table 1.1 places this thesis in the context with the previous studies. The main differentiation between this thesis and previous studies is the method of monitoring and controlling the temperature at the region for CNTs to grow. Previous studies have implemented the following techniques (either one or both):

(i) Numerical simulation of the relationship between the electric power and the induced temperature due to joule heating of the microheater [35, 37, 42, 43] .

(ii) Optical analysis of the black-body radiation [53] or Raman spectra [39] from the microheater to estimate the temperature.

The numerical simulation technique is not likely to provide high accuracy and repeatability. Dittmer *et al.* found that their simulation overestimated the temperature because their model had not correctly accounted for the heat transferred to the surrounding gases [43]. Moreover, their model had not included any additional changes in the thermal conductivity or other parameters due to physical or chemical changes in the microheater during synthesis. The optical analysis can provide a higher accuracy, however, it requires optical equipment and adds complexity to the synthesis process.

This thesis demonstrates a simple and robust method to control the synthesis temperature. The temperature at the center of the Si microheater (T) is monitored through *in-situ* measurements of the electrical resistance of the microheater (R). This method will be detailed in Chapter 3, section 3.2. Briefly explained, the resistance of a Si microheater is correlated with the temperature, since the resistivity of Si (doped) is highly sensitive to temperature. By means of experimental calibrations, the relationship between the input power (P) for heating the microheater and (R) and (T) was obtained. Since this P-R-T relationship is the nature of the Si microheater, it remains identical regardless of the changes in environment. This method uses only electrical signals, and allows for direct and fast feedback to control the input power in order to obtain a desired temperature. In addition, this method allows for a simple, automated, and parallel synthesis of CNTs

This thesis developed a process for the synthesis and integration of CNTs into Si microsystems that has the following characteristics: (i) Room-temperature environment; (ii) Localized growth and direct assembly of CNTs into the microsystems; (iii) Potential for batch fabrication at a low cost. After such a process, a two-terminal microsystem consisting of CNTs as the nano-functional element are produced. This system is referred as Si/CNTs/Si system in the following. The CNTs in Si/CNTs/Si systems are suspended and span the two Si microbridges. An example of a Si/CNTs/Si system is shown in Figure 1.3 (a & b). The as-fabricated Si/CNTs/Si systems were demonstrated to work as a NH_3 sensor, as presented in Figure 1.3 (c & d).

Table 1.1: Summary of previous studies on localized CVD synthesis and this thesis in context.

	UC Berkeley, USA[a]	ETH Zurich[b]	University of Edinburgh[c]	Other groups	This thesis
Device platform	SOI	PolyMUMPs	Metal on Si	CMOS; SOI; Glass; Metal on Si	SOI & PolyMUMPs
Localized parameter	localized heating	localized heating; localized catalyst	localized heating	localized catalyst; localized heating	localized heating
Microheater	Si	Poly-Si	W, Mo	Pt, Poly-Si, Si, Mo, Ti	Si & Poly-Si
Temperature indication	Optical analysis[d] *and/or* Numerical simulation[e]	Optical analysis *and/or* Numerical simulation	Optical analysis *and/or* Numerical simulation	Optical analysis *and/or* Numerical simulation	Evolution of resistance[f] & one-time calibration
Carbon source	C_2H_2, C_2H_4	CH_4	C_2H_2, C_2H_4	C_2H_2, CH_4,C_2H_4	C_2H_2
Carrier gas	None or Ar	None	Ar	Ar or H_2 or both or none	Ar
Catalyst preparation	*Evaporation* Fe, Ni, Mo	*Lithography + Solution drop-drying* $Fe(NO_3)_3$, Mo, Al_2O_3 particles.	*Evaporation* Fe, Mo, Ni	*Solution drop-drying*: $Fe(NO_3)_3$, Mo, Al_2O_3; *Evaporation*: Al, Fe-Ni-Co; *Sputtering*: Fe, Al_2O_3	*Evaporation* Fe, stacking Fe-Ni
Reference	[35–38, 53–56]	[32–34] for localized catalyst, and [57] for localized heating	[42–44]	for localized heating [39–41, 45, 46, 48–52] and for localized catalyst [58]	Articles listed in sec. 1.2.3. For stacking Fe-Ni, only article P1.

[a] Liwei Lin and co-workers (Englander, Christensen, Kawano, Chiamori, Sosnowchik, and more) at the University of California, Berkeley, USA. http://www.me.berkeley.edu/ lwlin/

[b] Christofer Hierold and co-workers (Jungen, Stampfer, Hoetzel, and more) at ETH Zurich, Switzerland. https://www.mavt.ethz.ch/people/professoren/chierold

[c] Eleanor E. B. Campell and co-workers (Dittmer, Mudgal and more) at the University of Edinburgh. http://www.ecampbell.chem.ed.ac.uk/index.html

[d] Optical analysis of the light emitted from the microheater (either black-body radiation [53] or Raman spectra [39]) to estimate the temperature.

[e] Numerical simulation of the relationship between the electric power and the induced temperature due to joule heating.

[f] The temperature of the microheater is monitored by only direct measurements of the electrical resistance of the microheater. The method will be detailed in Chapter 3, section 3.2.

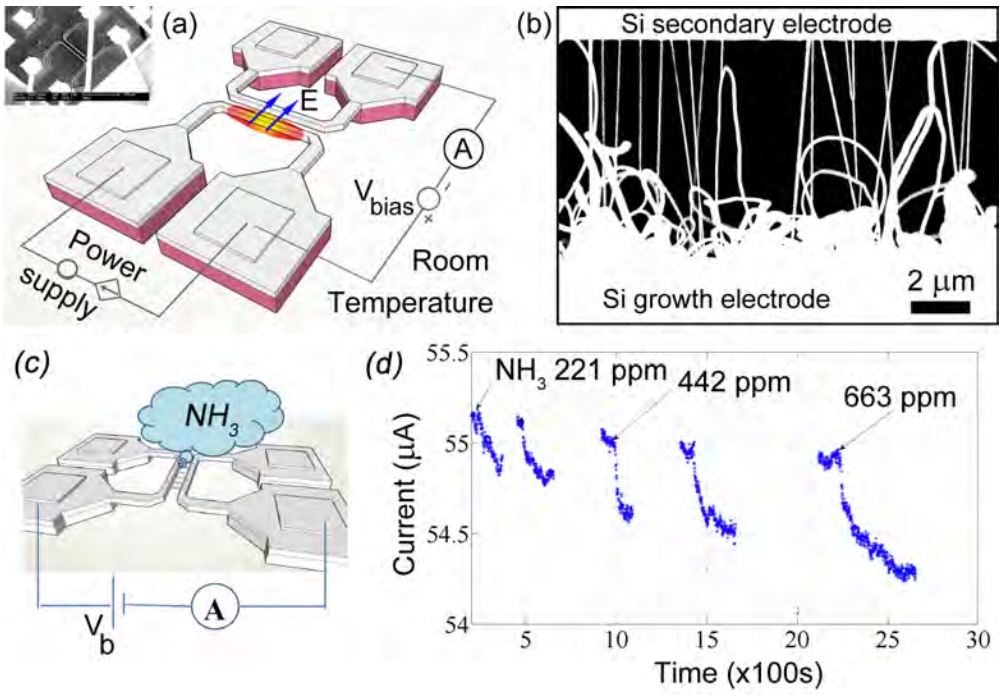

Figure 1.3: (a) Illustration of the local synthesis and direct integration of CNTs into microsystems; (b) SEM micrograph of a resulting Si/CNTs/Si system; (c) Circuitry for a NH_3 sensor experiment; (d) Response of a Si/CNTs/Si system to NH_3 [*Article P6*].

1.2 Research studies, contributions and publications

A list of research studies will be presented in the next section, followed by the lists of publications and contributions. Figure 1.4 show an overview of the research studies, in coupling with the contributions and publications.

1.2.1 Research studies

Study 1: Demonstrate a method of pure electrical control for the local synthesis and direct integration of CNTs into microsystem.

Study 2: Study the effects of synthesis conditions on the density, diameter, growth orientation and nanostructure of CNTs.

Study 3: Study the CNT-Si contacts: their structure and electrical behavior.

Study 4: Further develop the fabricated Si/CNTs/Si system for sensor applications.

Details about the studies will be presented in Chapter 3 to Chapter 6.

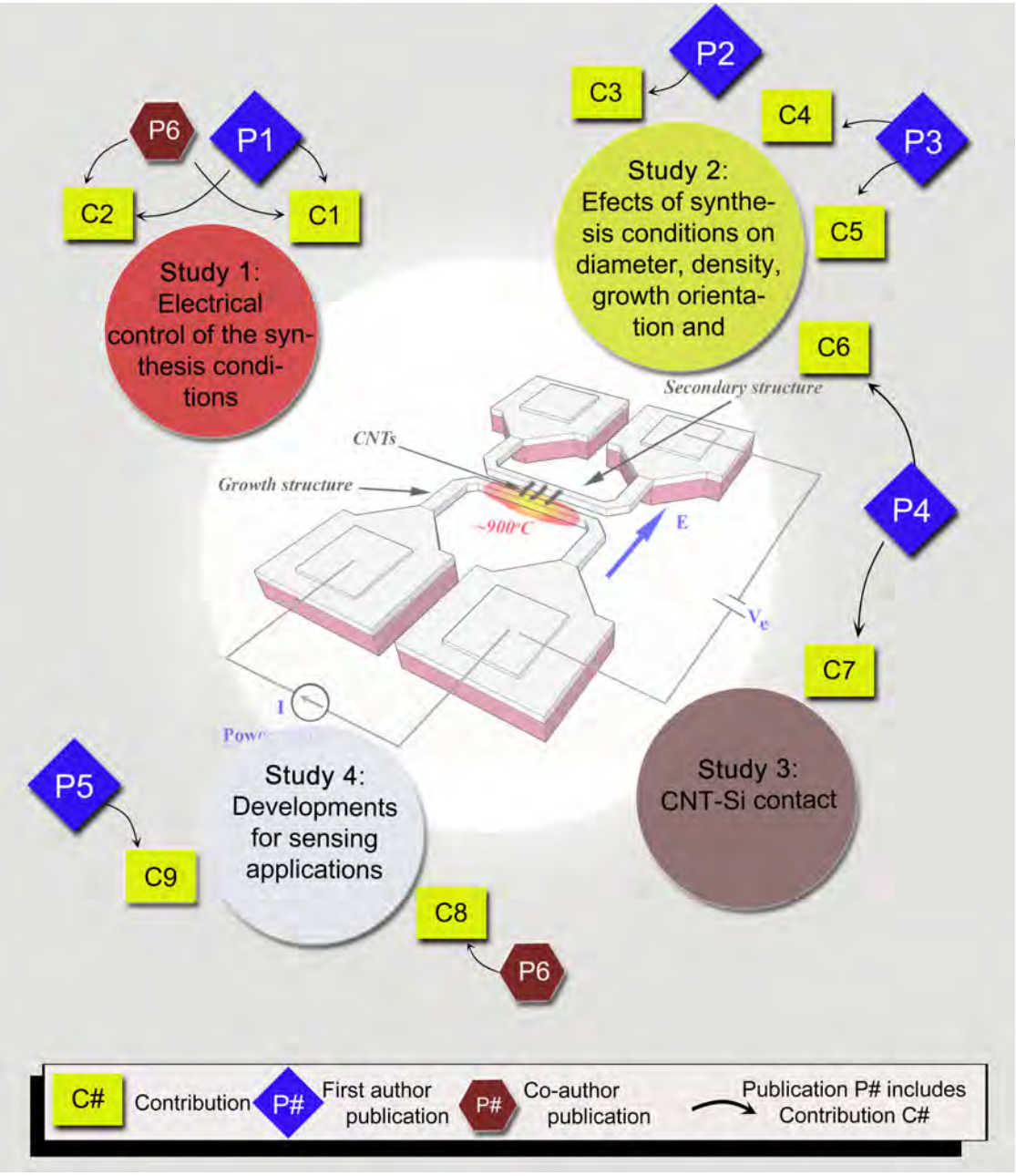

Figure 1.4: Distribution of publications with regard to studies and contributions of this thesis.

1.2.2 Contributions

Main contributions of this thesis are:

Contribution **C1**: A method of pure electrical control that enables a simple, automated and parallel process to synthesize locally and integrate directly CNTs into Si microsystems.

Contribution **C2**: A demonstration of the above method on polysilicon structures. Polysilicon is commonly used as a structural material of microelectromechanical systems (MEMS) and CMOS devices.

Contribution **C3**: A discovery of the diameter dependency for the electric-field assisted growth of CNTs.

Contribution **C4**: A discovery of the effect of local temperature on the resulting characteristics of locally grown CNTs.

Contribution **C5**: Microscopic observations of the structure of locally grown CNTs.

Contribution **C6**: High resolution SEM characterization with transmission mode imaging of the nanostructure of locally grown CNTs.

Contribution **C7**: Microscopic observations on the CNT-Si contact modes for locally grown CNTs.

Contribution **C8**: A demonstration of using a resulting Si/CNTs/Si system after synthesis as a NH_3 gas sensor.

Contribution **C9**: A demonstration of using thermal evaporation to functionalize the CNTs in the Si/CNTs/Si systems where CNTs are suspended and span two microelectrodes.

1.2.3 Publications

Papers are not available in this file due to publishers' restrictions

Publications enclosed in this thesis

P1: **Bao Q. Ta**, Nils Hoivik, Einar Halvorsen, and Knut E. Aasmundtveit, *"Electrical control of synthesis conditions for locally grown CNTs on polysilicon microstructure,"* Proceedings of the 11th IEEE Conference on Nanotechnology, 374-377, Portland, Oregon, USA, 15-18 Aug. 2011.

P2: **Bao Q. Ta**, Einar Halvorsen, Nils Hoivik, and Knut E. Aasmundtveit,, *"Diameter dependency for the electric-field-assisted growth of carbon nanotubes,"* Applied Physics Letters, 103, 123102-4, 2013.

P3: **Bao Q. Ta**, Tormod B. Haugen, Nils Hoivik, Einar Halvorsen, and Knut E. Aasmundtveit, *"Local Synthesis of Carbon Nanotubes in Silicon Microsystems: The Effect of Temperature Distribution on Growth Structure,"* Materials, 6, 3160-3170, 2013.

P4: **Bao Q. Ta**, Quoc-Huy Nguyen, Nils Hoivik, Einar Halvorsen, and Knut E. Aasmundtveit, *"Observations on defects and contact modes for locally grown CNTs,"* Proceedings of the 12th IEEE Conference on Nanotechnology, 1-6, Birmingham, UK, 20-23 Aug. 2012.

P5: **Bao Q. Ta**, Anh V. Ngo, Huy Q. Nguyen, Nils Hoivik, Einar Halvorsen, and Knut E. Aasmundtveit, *"Deposition of Palladium on Suspended and Locally Grown Carbon Nanotubes using Thermal Evaporation,"* Proceedings of the 13th IEEE Conference on Nanotechnology, 1176-1179, Beijing, China, 5-8 Aug. 2013.

P6: Knut E. Aasmundtveit, **Bao Q. Ta**, Liwei Lin, Einar Halvorsen, and Nils Hoivik, *"Direct integration of carbon nanotubes in Si microstructures,"* Journal of Micromechanics and Microengineering, 22, 074006, 2012.
My contribution: Did all experiments and all data analysis used in the paper, made all figures and contributed to the writing.

Publications not enclosed in this thesis:

During the time of my doctoral studies, I have also contributed to the following publications:

I. Knut E. Aasmundtveit, **Bao Q. Ta**, Quoc-Huy Nguyen, Tormod B. Haugen, Nils Hoivik, and Einar Halvorsen, *"Direct Integration of Carbon Nanotubes in Si Microsystems –Towards Truly Integrated Micro/Nano Systems,"* European Microelectronics Packaging Conference (EMPC), pp. 1-6, 9-12 Sept. 2013, Grenobe, France.

II. Knut E. Aasmundtveit, **Bao Q. Ta**, Nils Hoivik, and Einar Halvorsen, *"Electrical control on synthesis conditions for locally grown CNTs on polysilicon microstructures,"* Nanoelectronic Device Applications Handbook. CRC Press, Boca Raton, FL, USA, 2013.

III. Knut E. Aasmundtveit, **Bao Quoc Ta**, Quoc-Huy Nguyen, Tormod B. Haugen, Nils Hoivik, Einar Halvorsen, *"Local synthesis of carbon nanotubes for direct integration in Si microsystems-design considerations."* Advances in Manufacturing, **1**, *3*, 218-225, 2013

IV. Tormod B. Haugen, **Bao Q. Ta**, Einar Halvorsen, Nils Hoivik and Knut E. Aasmundtveit, *"Integration of carbon nanotubes in microsystems: Local growth and electrical properties of contacts."* Materials, **6**, *8*, 3094-3107, 2013.

V. Quoc-Huy Nguyen, **Bao Q. Ta**, Nils Hoivik, Einar Halvorsen, and Knut E. Aasmundtveit, *"Carbon Nanotube Based Gas Sensor for Expiration Detection of Perishable Food,"* Proceedings of the 13th IEEE Conference on Nanotechnology, 675-678, Beijing, China, 5-8 Aug. 2013.

VI. Heather Chiamori, Xiaoming Wu, Xishan Guo, **Bao Q. Ta**, and Liwei Lin, *"Annealing nano-to-micro contacts for improved contact resistance,"* Proceedings of the 5th IEEE International Conference on Nano/Micro Engineered and Molecular Systems (NEMS), 666-670, 20-23 Jan. 2010.

VII. Heather Chiamori, **Bao Q. Ta**, Knut E. Aasmundtveit, Liwei Lin, *"Activation and enhancement of carbon nanotube contacts using local electrical breakdown and thermal annealing,"* to be written.

Master theses under my co-supervision

1. A. V. Ngo, *"Functionalization of Carbon Nanotubes by Thermal Evaporation and Atomic Layer Deposition",* Department of Micro- and Nanosystem Technology, Vestfold University College (HiVe-IMST), Vestfold, Norway, 2013.

2. A. T. T. Nguyen, *"Direct Integration of Carbon Nanotubes in Microsystems: Reduction of Contact Resistance"*, Department of Micro- and Nanosystem Technology, Vestfold University College (HiVe-IMST), Vestfold, Norway, 2013.

3. T. B. Haugen, *"Synthesis and Characterization of Locally Grown CNTs",* Department of Micro- and Nanosystem Technology, Vestfold University College (HiVe-IMST), Vestfold, Norway, 2013.

1.3 Thesis structure

Chapter 2 will present the background of the CNT synthesis methods, the electrical properties, and sensor applications of CNTs. Each chapter from Chapter 3 to Chapter 6 will present a research study from Study 1 to Study 4 respectively. Chapter 7 will present the conclusion of this thesis. Finally, the published papers are enclosed.

Chapter 2

Background

2.1 Electrical properties of CNTs

2.1.1 Intrinsic properties

Both theoretical calculations and experiments have shown that electrical properties of CNTs are dependent on the diameter, chirality and structural disorder of the CNTs [59–61]. The chirality of a CNT can be expressed as the pair of indices (n,m) that indicates the direction of (conceptually) wrapping the graphene sheet to form the CNT. Calculations [59] predict that armchair CNTs (i.e. CNTs with n = m) are metallic. CNTs with n-m = 3N (N is an integer) are mostly metallic; otherwise, CNTs are semiconducting. Wilder *et al.* [60], using scanning tunnelling microscopy (STM) and spectroscopy, verified the theoretical prediction, and found that the bandgap (E_g) of semiconducting CNTs is around 0.4 - 2.0 eV and dependent on the tube diameter (d), $E_g \sim 1/d$. Odom *et al.* obtained similar results by STM measurements [61]. The band gap of MWNTs has been predicted to decrease with increasing tube diameter, and a MWNT with diameter d$\geq$10 nm is likely to be metallic rather than semiconducting [59]. Bachtold *et al.* [62], using electrostatic force microscopy and scanned gate microscopy, have found that:

(i) MWNTs with a diameter of 9 nm are diffusive conductors with a well-defined resistance per unit length ($\sim$10 kΩ/μm), while metallic SWNTs are ballistic conductors over micrometer lengths.

(ii) The resistance of a semiconducting SWNT is dominated by a series of strong scattering sites along the tube length. The origin of these scattering sites has not yet been found, but the authors proposed that it could correspond to the local defects in the nanotube or to the long-range electrostatic potential fluctuations associated with local charges or surface contaminants.

(iii) The authors obtained a value of $\sim$60 MΩ for the resistance of a bundle of semiconducting SWNTs (bundle diameter $\sim$3 nm, length $\sim$4 micrometers).

However, Li *et al.* [63] obtained a resistance between 150 kΩ - 6 MΩ for a semiconducting SWNT with a length of 20 μm (grown by CVD). The different results obtained by Bachtold *et al.* and by Li *et al.* probably result from the difference in the structure and disorder of the CNTs, since the electronic properties are strongly modulated by structural variations [64–69].

The electronic properties of CNTs can be manipulated. A p-type semiconducting CNT may be changed to behave as an n-type semiconductor by doping or annealing processes [70–73]. Derycke *et al.* found that a p-CNT field-effect transistor (FET) can be converted into an n-FET by annealing in a vacuum at 200°C for 10 hours. Bockrath *et al.* found that CNTs can change from p-type to n-type after being evaporated with potassium [73]. Conversely, an n-type CNT can become p-type after exposure to oxygen [71].

2.1.2 Contact between CNT and Silicon

An important issue that prevents the CNT-based devices from reaching their excellent electrical properties is the high contact resistance when connecting CNTs to the micro- and macro-structures. Kawano *et al.* [38] reported the resistance of a Si/CNT/Si system was ∼2.5 MΩ. The CNT in this system was a MWNT with a length of ∼7.5 μm and a diameter of ∼50 nm. According to Bachtold *et al.* [62], a MWNT with a diameter of 9 nm would have a resistance per unit length of ∼10 kΩ/μm and that nanotubes with larger diameters are more metallic. Thus, the intrinsic resistance of the above-mentioned CNT is expected to be less than ∼75 kΩ, which is one order of magnitude smaller than the total resistance of the Si/CNT/Si system (∼2.5 MΩ).

Schottky barrier exists at the CNT-Si contact, similar to the contacts between metal- semiconductor [74–76]. The Schottky barrier results in rectifying characteristics of the CNT-Si contact. In the contact between metallic CNT and n-type Si, the Schottky barrier hinders the electron flow from the CNT into silicon, but allows the opposite flow. If neglecting the Fermi-level pinning from interface states and barrier lowering from image charges, the barrier height Φ_B is equal to Φ_{CNT} - qχ [77]. The work function of CNT, Φ_B, is likely to be similar to graphite, which is 4.4 eV [78], and the electron affinity of silicon qχ is ∼4.0 eV [79]. The barrier height is thus about 0.4 eV. If the reverse bias is high enough for the breakdown to occur, the contact will be conducting; otherwise, there will no significant current. Using an avalanche breakdown model [80], we can estimate the reverse breakdown voltage for CNT-Si to be in the range 2 - 8 V when the doping concentration of n-type Si is on the order of 10^{18} cm^3.

The barrier height is dependent on the doping concentration of silicon [80, 81]. For heavily doped silicon, the barrier height is significantly reduced [77], the CNT-Si contact will then behave as an ohmic or near-ohmic contact. The metal-silicon junction model [81] suggests a specific contact resistivity of 10^{-5} - 10^{-8} Ωcm^2 for a MWNT-Si (*n*-doped) contact, using a barrier height of 0.4 eV and doping concentration of n-type Si at 10^{19} - 10^{20} cm^{-3}. For a CNT with a diameter of ∼30 nm and with tip-contact, the contact area is 10^{-12} - 10^{-11} cm^2. The calculated contact resistance for that CNT is thus in the range 10^7 - 10^3 Ω.

Not only the CNT-Si contacts, but also the CNT-Metal contacts have a high resistance. Liebau *et al.* reported that the contact resistance at the CNT-Metal interface is in the range 10^4 - 10^9 Ω [82–85]

2.2 CNT-based chemical gas sensor

2.2.1 Introduction

The electronic properties of SWNTs have been shown to be very sensitive to chemical environment [13]. Collins *et al.* [14] showed experimentally that the thermoelectric power (TEP) and electrical resistance of SWNTs can reversibly change upon exposure to a small amount of oxygen. Upon exposure to oxygen, semiconducting CNTs would apparently exhibit metallic behavior. The mechanism can be explained by using the nuclear magnetic resonance (NMR) study of SWNTs by Tang *et al.*: the spin-lattice relaxation rates of CNTs could increased dramatically upon exposure to oxygen and the fast relaxation is attributed to metallic characteristics [86].

Sumanasekera *et al.* [87] demonstrated experimentally that the electronic properties of SWNTs can be very sensitive to inert gases at temperature T>100 K. It was explained that the resistance change was caused either by the increased carrier scattering from dynamic defect states associated with momentarily adsorbed gas, or by the nonthermal, localized phonons generated by the collisions of gas molecules with the CNT wall.

Kong *et al.* found that semiconducting SWNTs changed their conductivity over several orders of magnitude under exposure to NO_2 and NH_3 at room temperature [88]. Within 10 seconds after exposure to 200 ppm NO_2, the conductivity of the SWNT increased by three orders of magnitude. Upon exposure to 1% NH_3, the conductivity of the SWNT decreased by two orders within 2 min. These responses were proposed to result from the charge transfer between the p-type semiconducting SWNT and the electron-donating NH_3 or electron-withdrawing NO_2 gas. When the SWNT absorbs (or adsorbs) NO_2 molecules, the NO_2 molecules withdraw electrons from the SWNT, thereby increasing the hole carrier concentration in the SWNT and causing an increase in conductance. The effect is opposite with NH_3 molecules: NH_3 molecules donate electrons to the SWNT, thereby reducing the hole carrier concentration in the SWNT and causing a decrease in conductance. Other gases with electron donating or accepting capabilities could also produce similar effects as NH_3 and NO_2. Oxygen can cause dramatic changes in resistance of CNTs [14]. Other gases, such as CO [89–91], CO_2 [92], CH_4 [93], ethanol [94–98], methanol [94, 99], acetylene [98], SF_6 [100], have been shown to be induce a change in the resistance of CNTs.

In general, existing chemical sensors use metal oxides and require a high temperature (up to 600°C) for the operations. In contrast, CNT-based sensors have significant responses at room temperature. However, CNT-based chemical sensors normally have a long recovery time (up to several hours) to release the analytes for another sensing operation. Poor recovery remains a drawback for CNT-based chemical sensors [88].

Table 2.1: Sensing performance of selected CNT-based chemical/gas sensors.

CNT type	Analytes	Detection limit	Reversibility[a]	Response time (s)	Reference
a single SWNT	NO_2, NH_3	2 ppm (NO_2) 0.1% (NH_3)	Irreversible	<600	Kong *et al.* [88]
SWNTs	O_2	Not-stated	Reversible	Not-stated	Collins *et al.* [14]
SWNTs	NO_2	44 ppb	Reversible (using UV light)	600	Li *et al.* [101]
MWNTs	NO_2	5-10 ppb	Reversible (at 165°C)	∼600	Valentini *et al.* [104]

[a] Reversibility: The quality of being recovered, i.e. releasing the analyte before another sensing operation.

Li *et al.* used a sensor that composes of CNTs network on an interdigitated electrode and obtained a short recovery time (to the order of minutes) by using ultraviolet light [101]. The authors found that the variation in sensitivity between devices was about 6%, indicating a superior reproducibility of CNT-based sensor to metal oxide or polymer-based sensors [102, 103].

The sensing performance of selected CNT-based chemical/gas sensors is shown in Table 2.1. Most CNT-based sensors are based on the change in the resistance of CNTs upon exposure to chemicals or gases. However, the sensor configurations are not limited to that. Alternative approaches have been demonstrated. Chopra *et al.* used a circular disk resonator coated with degassed CNTs, and found that the CNTs changed their dielectric constant upon exposure to CO, N_2, He, O_2 or Ar gas [90]. Their device achieved a sensitivity of ∼100 ppm, but required a relatively high temperature (125°C) and a low pressure (10^{-5} Torr) for operation. Ong *et al.* also used a CNT-based resonator to detect O_2 and CO, and showed that their sensors worked at room temperatures [92], thus indicating that the high temperature requirement is not insurmountable.

2.2.2 Role of defects on the sensing properties of CNTs

The sensing characteristics of CNT-based sensors can be improved, even modified, by introducing defects along the sidewall of the CNTs. Valentini *et al.* showed that defective CNTs exhibit a greater sensitivity toward NO_2 compared to defect-free CNTs [104]. Theoretical calculations predict that the defect sites on a CNT could result in a strong chemisorption and charge transfer to NO_2 molecules. Defect-free CNTs are normally less sensitive to gas molecule due to the strong sp^2 carbon-carbon binding in the CNTs. Robinson *et al.* introduced carboxylic acid sites on SWNTs, and observed an improved sensitivity to various analytes, such as acetone, methanol, hexane, toluene, H_2O [105]. The authors hypothesized that the increased adsorbate binding energy and charge transfer at the defect sites might im-

prove the sensitivity. Watts *et al.* studied the responses of pristine MWNTs and acid-treated MWNTs (treated by H_2SO_4/HNO_3 mixture) to water vapor and oxygen [106], and found that the acid-treated MWNTs had a higher sensitivity than the pristine MWNTs. The acid-treated MWNTs increased 5% in resistance after 100 seconds under exposure to H_2O vapor, while pristine MWNTs sensors increased only 3% in resistance. The authors explained that the oxygen-containing groups (e.g. the carboxyl -COOH) at defect sites withdraw electrons from the CNT, then increasing the hole carrier concentration in the CNT, and thus making the CNT become p-type semiconducting. Upon absorption of water molecules, the electron-withdrawing ability of these groups is reduced, thus causing a decrease in the hole carrier concentration, and accordingly causing an increase in the resistance of the CNT. Fu *et al.* [107] demonstrated experimentally that carboxylated SWNTs are also sensitive to CO, with a detection limit of 1 ppm, whereas pristine SWNTs did not respond.

2.2.3 Functionalization of CNTs with metal nanoparticles/nanoclusters

Pristine CNTs have a low specificity to different analytes, and have a low sensitivity to analytes that have a low affinity with CNTs. A solution for these shortcomings is to functionalize CNTs with functional groups. The binding between a functional group and CNT can be covalent or non-covalent, depending on the linkages of the functional groups. The esterification or amidation of carboxylic acid groups during acid treatment of CNTs can form functionalized CNTs with covalent bonds [108, 109]. Functionalized CNTs that have non-covalent bonds with the functional groups can be formed by supramolecular complexation due to adsorptive and wrapping forces, such as van der Waals and π-stacking interactions [110, 111]. Most studies about the functionalization of CNTs for gas sensors used either organic polymers or metal nanoparticles/nanoclusters. CNTs could also be functionalized with organic polymers, but this is out of scope of this thesis, thus not being reviewed further.

Kong *et al.* demonstrated that SWNTs functionalized by electron-beam evaporation of Pd (target thickness:$\sim$0.5 nm) are excellent for detection of hydrogen at ambient conditions, with a fast response, a high sensitivity and a high reversibility [88]. The authors reported that the electrical resistance of the Pd-decorated SWNTs doubled when the SWNTs were exposed to 400 ppm H_2. Their proposed mechanism is that H_2 molecules dissociate into hydrogen atoms at the surface of a Pd nanoparticle, and dissolve into the particle, and then inducing a decrease in the work function of Pd. As a result, more electrons can transfer from Pd to SWNT. As the SWNT was p-type semiconducting, the hole carrier concentration in the SWNT will be reduced when more electrons transfer from Pd to the SWNT, and hence the resistance of the SWNT will increase. The response time of Pd-decorated SWNTs was 5-10 s, and the recovery time was $\sim$400 s. The sensor is reversible, because hydrogen atoms in Pd can combine with O_2 in air to form H_20 that leave off the SWNT, thus recovering the initial resistance.

Kumar *et al.* demonstrated good H_2 sensors at room temperature, using MWNTs that were chemically functionalized with Pt and Pd nanoparticles [112]. The formation of Pt (or Pd) nanoparticles on MWNTs was realized by a solution treatment, using H_2PtCl_6 or $PdCl_2$ and a reduction agent such as $NaBH_4$. The functionalized MWNTs had a high sensitivity and a

high reversibility at room temperature to H_2 gas. The authors proposed a mechanism that was similar as proposed by Kong *et al.*, presented in the previous paragraph.

The CNTs functionalized with Pd nanoparticles also have a good sensitivity to CH_4, as demonstrated by Lu *et al.* [113]. The deposition of Pd nanoparticles onto CNTs were realized by sputtering of Pd with a target thickness of 10 nm. The authors found that Pd-decorated CNTs can detect CH_4 at a concentration of 6-100 ppm. The resistance of Pd-decorated CNTs reduced upon exposure to CH_4; this is opposite to the case of H_2. The authors proposed a mechanism that hydrogen atoms in CH_4 withdraw electrons from Pd, resulting in more hole carriers in the CNT. For p-type semiconducting CNTs, this effect will result in a decrease the resistance of the CNTs. Most as-grown SWNTs were p-type semiconducting.

Sayago *et al.* demonstrated a solution-based method for the functionalization of CNTs with Pd [114]. The authors used a palladium salt and used toluene as a solvent. Pd nanoparticles (sizes of 3-10 nm) were uniformly attached to CNT sidewall. The resulting Pd-decorated CNTs had good response to H_2 at a concentration of 0.1%-2%, at room temperature.

Mubeen *et al.* used site-specific eletrodeposition technique to functionalize CNTs with Pd [115]. The functionalized CNTs had a good sensitivity to H_2 (0.42% resistance change per ppm) with a detection limit of 100 ppm. Their sensors exhibited a linear response up to 1000 ppm at room temperature, but had a poor reversibility in Argon environment. The author found that their sensors response faster in humid air conditions than in dry air conditions.

Young *et al.* [116] fabricated NO_2 sensors using a SWNT thin-film coated with alkanethiol-monolayer-protected gold clusters. Their sensors can detect NO_2 at a concentration of 4.6 ppb at ambient conditions. The authors used ultraviolet light to accelerate the recovery process of their sensors (i.e. to improve the reversibility).

Penza *et al.* functionalized MWNTs bundles with Au- or Pt- or Pd-nanoclusters for the detection of NO_2, NH_3, H_2S, and CO [117, 118]. The MWNTs bundles were synthesized by plasma-enhanced CVD on an alumina substrate. Pt- (and Pd-) nanoclusters were deposited on the surface of the MWNTs by sputtering of Pd (and Pt) with a nominal thickness of 5 nm. The authors found that the Pd- and Pt-functionalized CNTs had superior sensing characteristics, as shown in Table 2.2.

Functionalized CNTs are great elements of a sensor network that can detect different gases at the same time. In such a sensor network, each sensor has a high sensitivity and selectivity to a specific analyte. Star *et al.* fabricated a sensor array consisting isolated, individual CNT-based sensors [119]. Each sensor was functionalized with a specific metal, such as Au, Pt, Pd, or Rh. The functionalization was realized by site-selective electrochemical deposition. A resulting sensor array could detect different gases: H_2, CH_4, CO, H_2S, NH_3 and NO_2. A combination of pristine CNTs, Au-decorated CNTs, Pd-decorated CNTs, and polymer-coated CNTs have been demonstrated by Lu *et al* [120]. The authors fabricated a sensor array by combining thirty-two CNT-based sensors. This sensor array could detect NO_2, HCN, HCl, Cl, acetone and benzene at a concentration on the order of ppm. This sensor array also successfully discriminated the targeted gases. Table 2.3 presents a summary of selected literature on CNT-based sensors using metal-funcationalized CNTs.

Table 2.2: Sensing performance of Pd- and Pt-functionalized CNTs towards NO_2, NH_3, H_2S, and CO at a temperature of 200°C - reported by Penza *et al.* [117].

Test gas	Mean sensitivity (%/ppm)[a]			Detection limit[a]		
	CNTs	Pd-CNTs	Pt-CNTs	CNTs	Pd-CNTs	Pt-CNTs
NO_2	3.2	3.8	3.9	19 ppb	9 ppb	3 ppb
H_2S	1.3	1.6	3.7	46 ppb	23 ppb	4 ppb
NH_3	0.008	0.02	0.07	3.8 ppm	1.7 ppm	0.2 ppm
CO	0.0007	0.0012	0.0039	90 ppm	32 ppm	4 ppm

[a] Mean sensitivity is defined as $S_m = \frac{1}{n}\sum_{i=1}^{N}\frac{(\Delta R/R)_i}{c_i}\,(\%/ppm)$, where $(\Delta R/R)_i$ is the percentage relative change in resistance corresponding to the i^{th}-measurement for gas concentration c_i, for N exposures to the same gas.

Table 2.3: Sensing performance of selected metal-functionalized CNT sensors.

Metal	CNT type	Target gas/vapor	Functionalization method	Detection limit	Response time (s)	Reference
Pd	a single SWNT	H_2	Electron-beam evaporation	40 ppm	5-10	Kong *et al.* [88]
Pd	SWNTs	H_2	Chemical solution; Sputtering	1000 ppm	Not stated	Sayago *et al.* [114]
Pd	SWNTs	CH_4	Sputtering	6 ppm	120-240	Lu *et al.* [113]
Au, Pd, Pt	MWNTs	NO_2, NH_3, H_2S, CO	Sputtering	3 ppb (NO_2), 4 ppb (H_2S), 0.2 ppm (NH_3), 4 ppm (CO)	<600	Penza *et al.* [117, 118]
Au	SWNTs	NO_2	Drop-coating mono-layer Au clusters	4.6 ppb	Not-stated	Young *et al.* [116]
Pd	SWNTs	H_2	Electrochemical functionalization	100 ppm	600	Mubeen *et al.* [115]
Pt, Pd	MWNTs	H_2, NO_2, H_2O	Chemical functionalization	Not-stated	600-1800	Kumar *et al.* [112]
Pt, Pd, Sn, Rh	SWNTs	H_2, CH_4,CO, H_2S	Electrochemical deposition; E-beam evaporation	Not-stated	600	Star *et al.* [119]

2.3 Bulk synthesis of CNTs

2.3.1 Arc Discharge

The discovery of CNTs were from an arc discharge experiment [1] by Iijima in 1991. Figure 2.1 shows the schematic of the Arc Discharge synthesis of CNTs. A high temperature up to $\sim$4000°C) is created by passing a DC current (50 - 100 A) through two graphite electrodes (at a separation of $\sim$1 mm. The discharge occurs and vaporizes the surface of one graphite electrode (the anode), producing carbon vapors. The carbon atoms will then deposit at the other electrode (the cathode), forming CNTs and various carbon products [1, 19–22].

The arc discharge technique can produce both SWNTs and MWNTs, depending on the composition of the anode. If the anode is pure carbon, MWNTs are produced [121, 122]. If the anode contains metal catalysts, SWNTs are produced [19,123,124]. The reaction atmosphere is a parameter to control the CNT diameter [20].

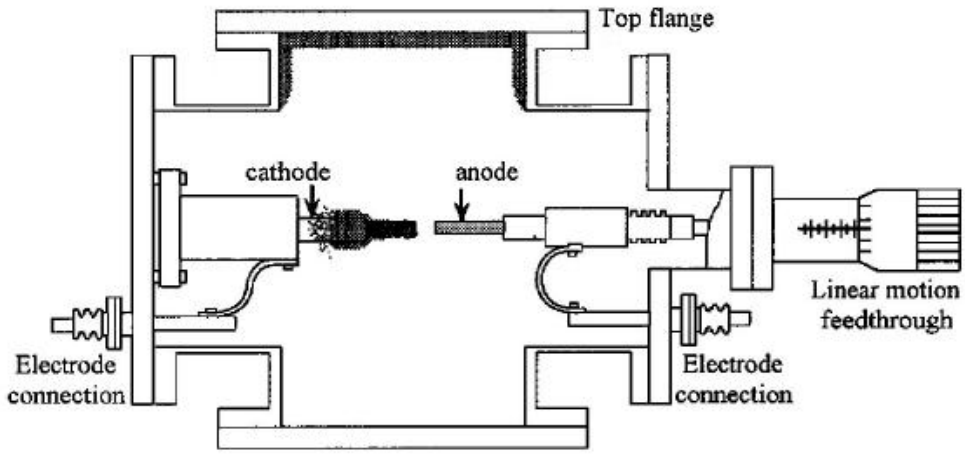

Figure 2.1: Schematic of the Arc Discharge synthesis of CNTs [19]. A direct current of 50 to 100 A, driven by a potential difference of approximately 20 V, creates a high temperature between two electrodes of carbon rods at a separation $\sim$1 mm. The discharge vaporizes the surface of one of the carbon electrodes. The carbon vapors condenses at the other electrode, forming CNTs and various carbon products.

2.3.2 Laser Ablation

In Laser Ablation, a laser beam is used to vaporize the carbon source in an inert gas environment [23], at a temperature of 800-1200°C. The laser converts a small amount of the carbon source into a plasma of carbon atoms and molecules. CNTs together with various products will be produced in the plasma plume, and then follow the carrier gas to deposit at the end of the chamber [23–28]. Examples of laser sources used in Laser Ablation are CO_2 lasers [27,28,125] and Nd:YAG [24,125] lasers, either in continuous [27] or pulsed [125,126] operation. Figure 2.2 shows a simple schematic of an apparatus for Laser Ablation synthesis

of CNTs. Both MWNTs and SWNTs can be produced by Laser Ablation. MWNTs will be the main product if the carbon source is pure graphite or boron-doped graphite [127]. SWNTs will be the main product if f the carbon source is doped with metal catalyst (such as nickel, or cobalt) [23, 128–130].

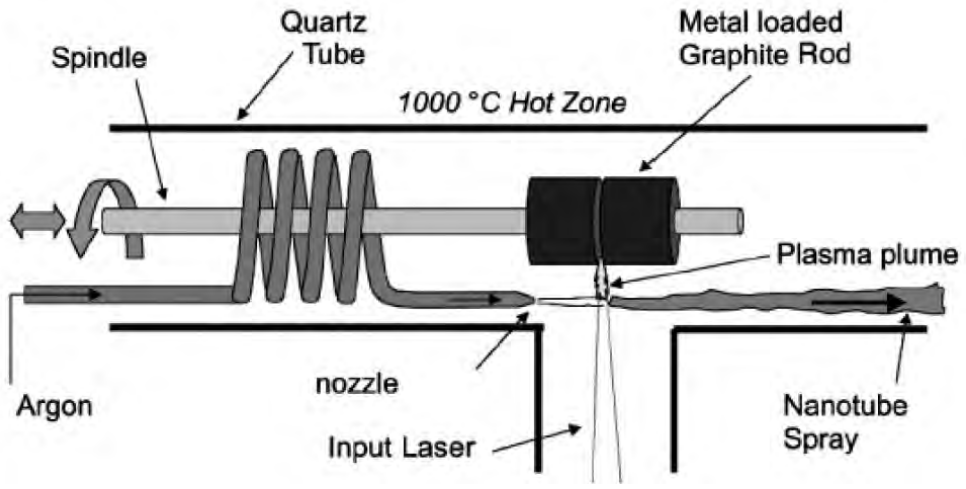

Figure 2.2: Typical apparatus for the Laser Ablation synthesis of CNTs [126]. The laser converts a small amount of the carbon source into a plasma of atoms and molecules. In the plasma plume, carbon atoms will bind together and form CNTs and various carbon products.

2.3.3 Chemical Vapor Deposition (CVD)

Chemical vapor deposition (CVD) has become the most popular method for the synthesis of CNTs. CVD growth of CNTs involves in the decomposition of a carbon-containing gas or vapor (e.g. C_2H_2) at high temperature and presence of a metal catalyst. CVD growth of CNTs was first demonstrated by Endo *et al.* in 1993 [29], although Baker *et al.* had demonstrated the formation of carbon filaments by the decomposition of C_2H_2 in 1972 [131].

CVD has become the most widespread method since it has a relatively low cost, a large-scale capability, a high versatility. Many variations of CVD techniques have been developed, including thermal CVD (or conventional CVD) [30], plasma-enhanced CVD [31], water-assisted CVD, [132, 133] , oxygen-assisted CVD [134], hot-filament CVD (HF-CVD) [135], microwave plasma CVD (MPE-CVD) [136, 137] or radio-frequency CVD (RF-CVD) [138]. Each technique has advantages and disadvantages in terms of purity of the product, cost, scalability, controllability.

Thermal CVD

Thermal CVD has high versatility, simplicity and wide process window of parameters. Compared to other methods (e.g. plasma-enhanced CVD, oxygen-assisted CVD, etc.), thermal CVD offers relatively inexpensive equipment and reactants. Generally, a thermal CVD process is conducted in a reaction chamber held at a temperature of 550 - 1200^{o}C [139, 140]. A

mixture of carbon source gas (or vapor) and a carrier gas is fed into a reaction chamber for the growth of CNTs. The carbon source gas is normally a hydrocarbon, such as acetylene (C_2H_2), ethylene (C_2H_4), benzene (C_6H_6), methane (CH_4), etc. [141–143]. The carrier gas is normally an inert gas, such as nitrogen, helium, or argon. The carbon source molecules will be decomposed by either the catalytic action of metal nanoparticles or by self-pyrolysis, at elevated temperatures. For instance, pyrolysis of benzen in the presence of Ni catalyst occurs at 900°C, and in the absence of Ni catalyst it occurs at 1140°C [144]. In CVD, the growth of CNTs require the presence of catalyst nanoparticles; otherwise, other carbon products will be formed. CNTs grow from the catalyst nanoparticles, since the decomposition of carbon-source molecules occurs at the surface of the catalyst particles. A simple schematic of a thermal CVD apparatus is shown in Figure 2.3

Catalyst is a critical factor in CVD growth of CNTs. Common catalyst are metal nanoparticles, such as Fe, Ni, Mo, Co and most of transition metals. The catalyst is typically deposited on the substrate surface prior to the growth reaction, but can also be fed into the reaction chamber simultaneously with the carbon source. The type and amount of catalyst affect the yield, structure and diameter of CNTs [145–147]. CNTs grown by CVD commonly have a higher degree of defect and disorder than CNTs grown by Laser Ablation or Arc Discharge.

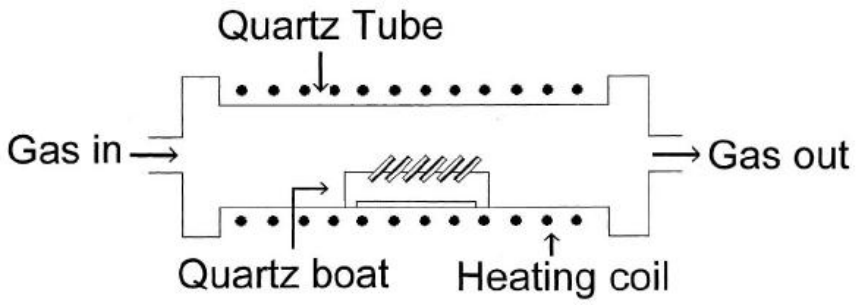

Figure 2.3: Schematic of an apparatus for thermal CVD growth of CNTs [124]. The heating coil provides high temperature for the decomposition of the carbon source gas at the metal catalyst particles. Carbon atoms bond together and grow CNTs from the metal particles.

2.4 Localized CVD synthesis

Common CVD techniques require a high temperature reaction chamber for the CNT synthesis, and require additional processes to maneuver and assembly CNTs into a device after synthesis [148–150]. The transferring processes are normally complicated and time-consuming. The high temperature requirement hinders the direct integration of CNTs into devices. Solutions for these problems would be to either localize the thermal environment or the catalyst position or both.

The approach of localizing the catalyst position allows for the direct integration of CNTs into a device, since it allows for CNTs to grow only at specific locations [32–34, 151]. Jungen *et al.* [32] reported a process flow consisting of 5 main step: (i) Spin coating photoresist PMMA on a 2 mm $\times$ 2 mm chip that contains PolyMUMPs microsystems; (ii) Electron

beam lithography to create openings with a feature size of 2 μm, which will serve as place-holders for the catalyst; (iii) a droplet of iron nitride dissolved in methanol is placed onto the chip, followed by a drying process; (iv) lift-off process to strip PMMA away, leaving islands of iron nitride at the defined place-holders; (v) CVD growth of CNTs (in a furnace at 900°C at ∼75 Torr, using CH_4 as carbon feedstock); (vi) metallization (deposition of metal for electrical connections); (vii) HF release and CO_2 drying. The authors successfully fabricated microsystems that contain CNTs as the active element. Dong *et al.* [58] also used electron beam lithography to define the locations of catalyst (nickel), and achieved better confinement of catalyst islands (in size of 50-150 nm). In general, the approach of localizing the catalyst position solves only the problem of direct placement and assembly of CNTs into a device.

In many cases, the device may contain temperature-sensitive materials that can be altered or even destroyed at high temperature. For example, processed CMOS devices should not be exposed to a temperature above 300-400°C. In such case, localizing only the catalyst position is not enough. The thermal environment needs to be localized. In fact, when the thermal environment is localized, both the problems of high temperature and direct assembly are solved. The approach of localizing the thermal environment was first demonstrated by Englander *et al.* [35]. The authors used a suspended Si microbridge as a microheater, which is locally heated by the passage of an electric current (Joule heating) to provide a hot region for the growth of CNTs. Their experimental setup is illustrated in Figure 2.4. The growth of CNTs occurred when the microheater is heated to about 850-900°C in the presence of a carbon source gas (C_2H_2 or C_2H_4) and catalyst nanoparticles. The induced temperature was monitored through an analysis of the light emitted from the microheater (and one-time calibration by temperature-indicating paint). The utilization of Si microheaters for localized heating has also been demonstrated by other researchers [39, 41]. This is also the scheme used in this thesis.

In a different route, Dittmer *et al.* used metals (W or Mo), instead of Si, for the micro-heaters [42–44]. The metal microheaters were patterned directly on a Si wafer by using standard photolithography, lift-off, and electron beam evaporation. The authors monitored the induced temperature based on modeling and *in-situ* analysis of black-body radiation from the heater. Lin *et al.* used Ti/Au microheaters, and also used modeling to control the induced temperature [46]. Zhou *et al.* used Pt microheaters to locally synthesize and directly integrate SWNTs into a CMOS system. During synthesis, the temperature of the heater was estimated based on the applied voltage. The relationship between temperature and voltage was characterized by using infrared imaging technique.

The approach of localizing the thermal environment is not limited to resistive heating. Other methods, such as laser-assisted heating [47, 49], plasmon-assisted heating [51, 52], induction heating [53, 152] have also been demonstrated.

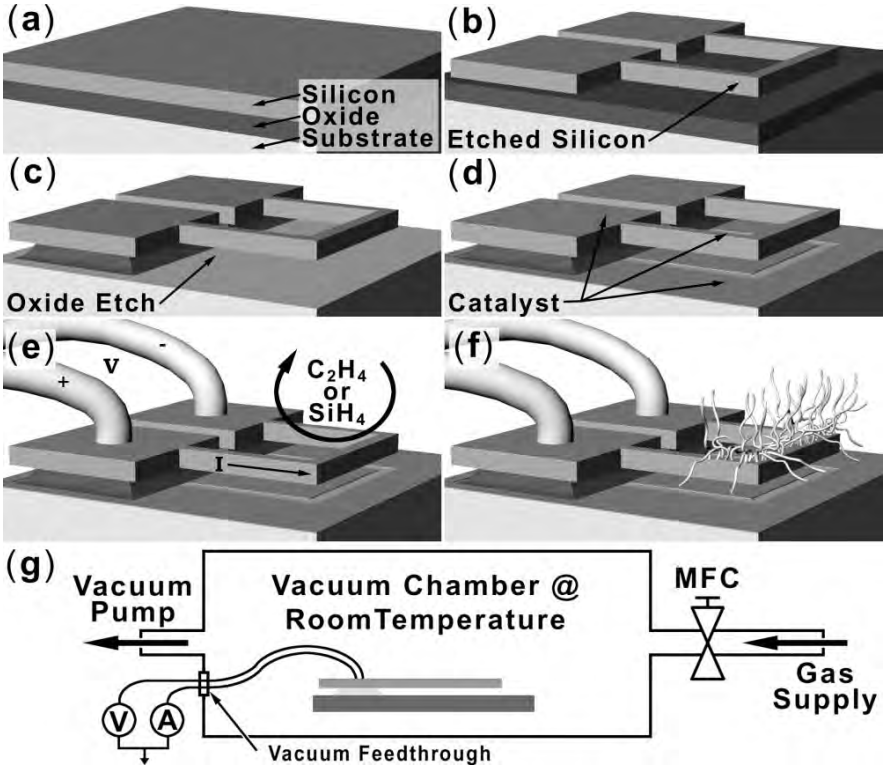

Figure 2.4: Local synthesis of CNTs or Si nanowires, using resistive heating for localizing the high temperature region, demonstrated by Englander *et al.* [35]. (a) Initial SOI (Silicon-on-Insulator) wafer. (b-c) Microstructure fabrication. (d) Maskless evaporation of metal catalyst. (e) Wirebonds and electrical supply. (f) Resulting nanostructures (CNTs or Si nanowires). (g) Schematic of the experimental setup in a chamber at room-temperature.

Laser-assisted heating is realized by focusing a laser beam onto a catalyst-coated surface, producing a localized hot spot for the CVD growth of CNTs [47–50, 153].

Plasmon-assisted heating is realized when the metal catalyst particles are illuminated by a laser with a wavelength close to the plasmon resonant frequency of the metal. The laser excites surface plasmons in the metal particles, causing localized heating [51, 52].

Induction heating is realized by Eddy currents generated in a conducting substrate due to a high-frequency magnetic field. The induced Joule heating could be confined within several microns depths of the substrate [53].

The resistive heating method requires simpler experiment setups than other methods, as the other methods require a laser and a transparent chamber that allows laser to illuminate the microstructures.

Chapter 3

Design and Fabrication

The method of local synthesis and direct integration of CNTs is demonstrated on Si microsystem. A microsystem consists of two suspended Si microelectrodes. After the synthesis and integration process, a two-terminal microsystem that contains CNTs as the nano-functional element is produced. The resulting microsystem (referred as Si/CNTs/Si system) could work as a gas sensor.

The Si microsystems was fabricated by using commercial PolyMUMPs and SOIMUMPs platforms. Such platforms were chosen to demonstrate that CNT-based device fabrication is commercially feasible. PolyMUMPs is a *three-layer polysilicon surface micromachining process*. SOIMUMPs is a *silicon on insulator (SOI) micromachining process* [154, 155]. Figure 3.1 shows the cross-section view of PolyMUMPs and SOIMUMPs structures. In a PolyMUMPs microsystem, there are three structural layers made of polysilicon. In a SOIMUMPs microsystem, there is one structural layer made of single-crystalline silicon.

PolyMUMPs microsystem is the focus of this thesis, because polysilicon is commonly used as the structural material for MEMS and CMOS devices. SOIMUMPs microsystem is an alternative that enables direct characterization of CNTs by the transmission mode imaging of a high-resolution SEM, because SOIMUMPs platform allows for making a through-hole in the Si substrate below the microelectrodes where CNTs grow.

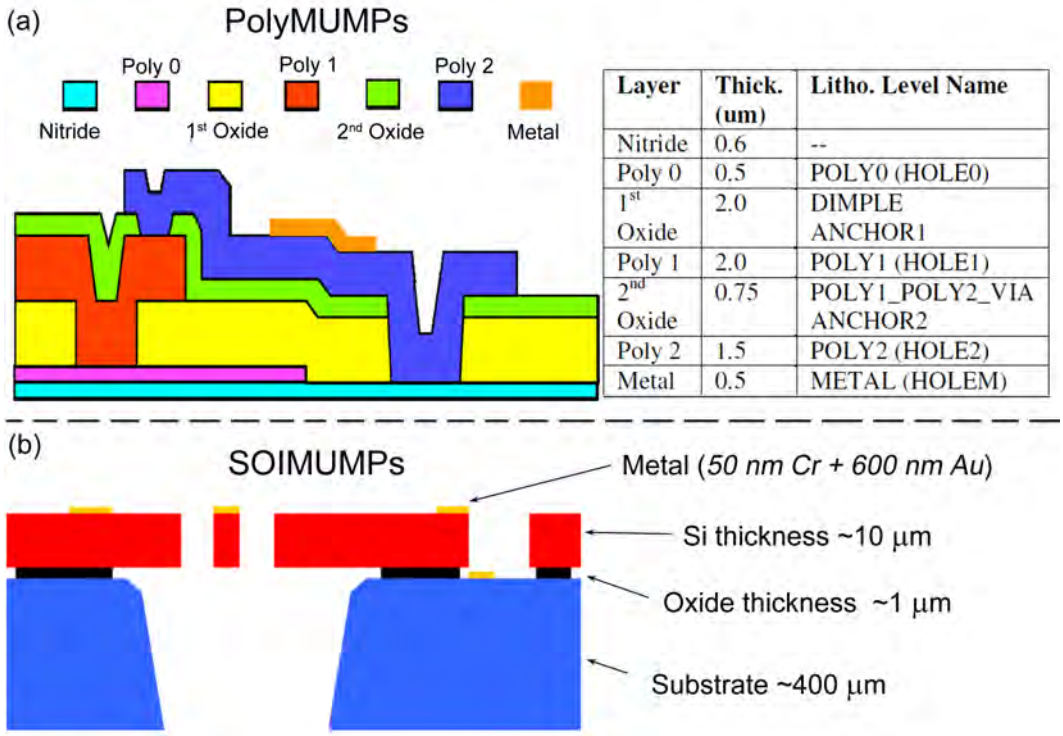

Layer	Thick. (um)	Litho. Level Name
Nitride	0.6	--
Poly 0	0.5	POLY0 (HOLE0)
1st Oxide	2.0	DIMPLE ANCHOR1
Poly 1	2.0	POLY1 (HOLE1)
2nd Oxide	0.75	POLY1_POLY2_VIA ANCHOR2
Poly 2	1.5	POLY2 (HOLE2)
Metal	0.5	METAL (HOLEM)

Figure 3.1: Cross-section view showing all layers of the PolyMUMPs (a) and SOIMUMPs (b) microsystems.

3.1 Design of the microsystem

3.1.1 PolyMUMPs microsystems

Basic design

A basic microsystem simply consists of two suspended Si microelectrodes. Each electrode is a micro rectangular bar of Si, being elevated above the substrate. The microbar is supported by two hanging arms, connecting to the anchors, as depicted in Figure 3.2. The feature dimensions are presented in Table 3.1.

The width of the microelectrodes is an important factor, as it defines the region for the CNT growth. A narrow microelectrode is favorable, since it provides a better confinement of the location of CNTs. Because the minimum feature width in PolyMUMPs is 2-3 µm [154], with a safety margin, a width of 5 µm was chosen for the microelectrodes. Two variations were: 10 and 15 µm.

The length of the electrode (excluding the hanging arms) was chosen to be 160 µm, since the size of contact pads is ∼130 µm and the separation between the pads required for wire bonding is ≥30 µm.

The thickness of the microelectrodes can be either 2.0 µm or 3.5 µm [154]. Both options have been investigated. It was found that most 2.0-µm-thick microelectrodes bent down and

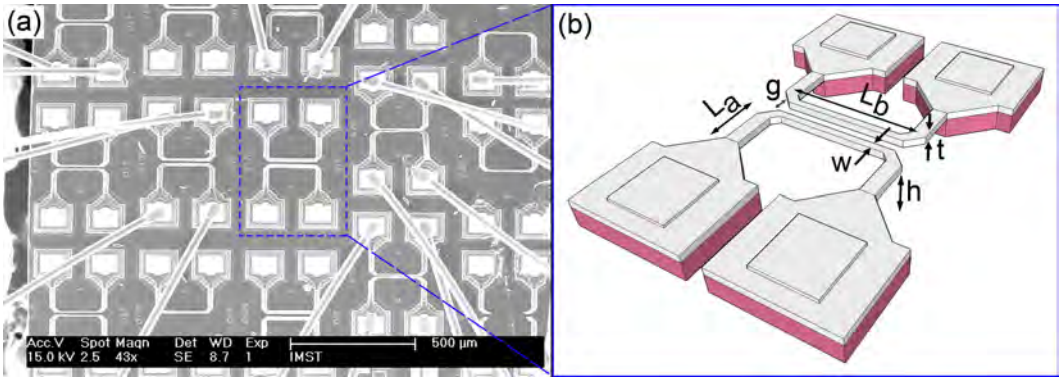

Figure 3.2: Basic design of the microsystems for demonstrating the method of local synthesis and direct integration of CNTs into Si microsystems. Each microsystem consists of two suspended Si microelectrodes. (a) Overview of an entire PolyMUMPs chip. (b) Sketch of a microsystem. Selected dimensions will be presented in Table 3.1

Table 3.1: Dimensions of the basic microsystem shown in Figure 3.2

Dimension	Symbol	Values
Width at the region for CNT growth	w	5, 10, 15 μm
Length of the region for CNT growth	L_b	160 μm
Structural thickness	t	3.5 μm
Height above the substrate	h	2 μm
Separation between two microelectrodes	g	5, 10, 15 μm
Length of the supporting arm	L_a	60 μm

touched the substrate, whereas all 3.5-μm-thick microelectrodes were suspended above the substrate and did not bent. Note that during the synthesis of CNTs, a microelectrode will be locally heated (using Joule heating) to provide a localized hot region for CNTs to grow. Thus, the microlectrodes need to be suspended to avoid the heat transfer directly to the substrate.

Saw-like microelectrode

One of microelectrodes has pointing tips, as shown in Figure 3.3. The electrode looks like a saw, thus being named "Saw-like microelectrode". This design is useful to investigate the effect of an electric field on the growth orientation of CNTs. The local electric field between the two electrodes, established by a bias voltage between them, would concentrate at the pointing tips. If the growth orientation of CNTs follows the electric field, the CNTs will also concentrate at the pointing tips. Results will be presented in Chapter 4, section 4.3).

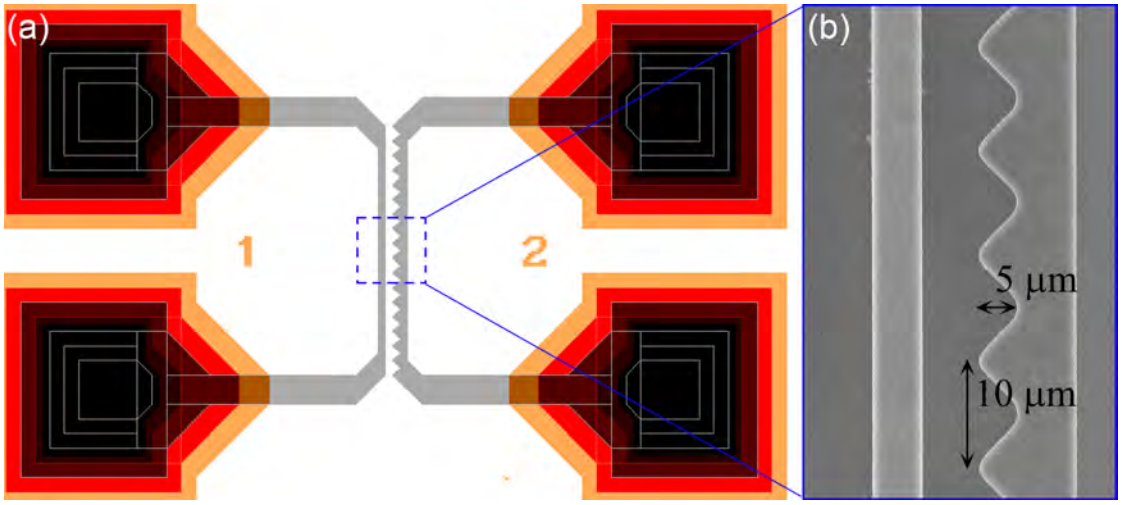

Figure 3.3: (a) Design of a microsystem with a saw-like microelectrode. (b) SEM micrograph of such a microsystem at the marked area in (a).

3.1.2 SOIMUMPs microsystems

SOIMUMPs platform allows for making a through-hole in the Si substrate below the growth region of CNTs. This through-hole allows for the transmission mode imaging directly on the fabricated Si/CNTs/Si systems, as shown in Figure 3.4. The Hitachi S-5500 S(T)EM at NTNU Nanolab, Trondheim, Norway was used. The S(T)EM imaging of CNTs was performed directly on the Si/CNTs/Si microsystem after the synthesis process, without need for complicated steps of sample preparation.

The design of SOIMUMPs microsystems was studied in a master thesis under my co-supervision (T. B. Haugen [156]). This thesis used these microsystems for the synthesis and integration of CNTs, and the S(T)EM characterization of CNTs.

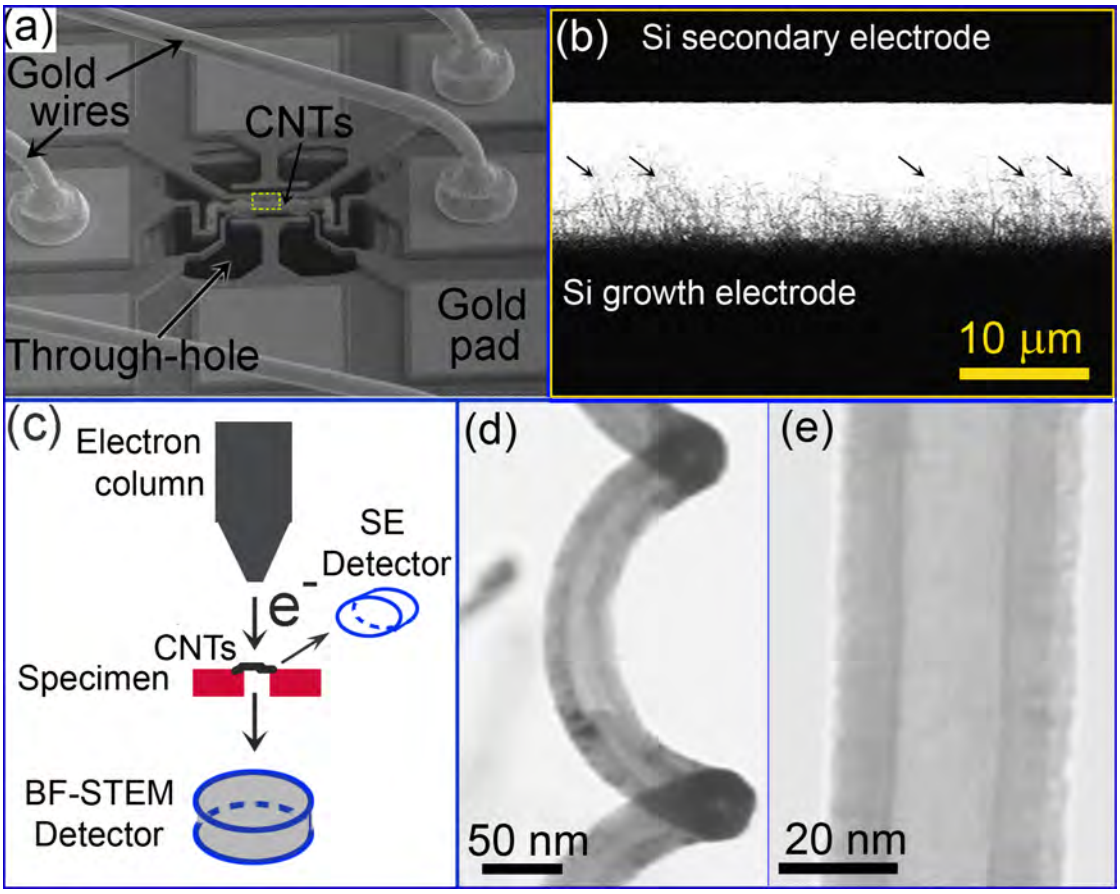

Figure 3.4: (a) SE-SEM image at 5 kV of an SOIMUMPs microsystem. (b) BF-S(T)EM image at 30 kV of the region in-between the two microelectrodes of a microsystem; (c) Illustration of the transmission mode imaging of locally grown CNTs by using the Hitachi S-5500 S(T)EM; (d) BF-S(T)EM image at 30 kV of a helical CNT and (e) a straight CNT. Abbreviation: SE = Secondary Electron, BF = Bright Field.

3.2 Synthesis process

The process of local synthesis and direct integration of CNTs into a Si microsystem is briefly described as follows. Prior to the synthesis process, a thin layer of Fe (thickness 3-5 nm) was deposited on the microsystem by maskless thermal evaporation. During the synthesis, one microelectrode (referred to as "growth electrode") was locally heated by the passage of an electric current (Joule heating) to induce a temperature of 900°C at the center of the electrode. At this temperature, the Fe layer transforms into Fe nanoparticles, which serve as catalyst particles for the growth of CNTs. A mixture of acetylene (C_2H_2) and a carrier gas (Argon), both at a flow rate of 50 cm^3 per minute (ccm), was then introduced to the reaction chamber to initiate the CNT growth. C_2H_2 molecules decomposed into carbon atoms at the surface of a catalyst nanoparticle; the carbon atoms then bound together and formed CNTs. To assist CNTs grow towards the other microelectrode (referred to as "secondary electrode"), a local electric field was established by using a bias voltage between two microelectrodes. The circuitry is shown in Figure 3.6. A self-made Labview program was used to control the synthesis conditions: gas flow rates, electrical power for heating the growth electrode, electrical *in-situ* measurements.

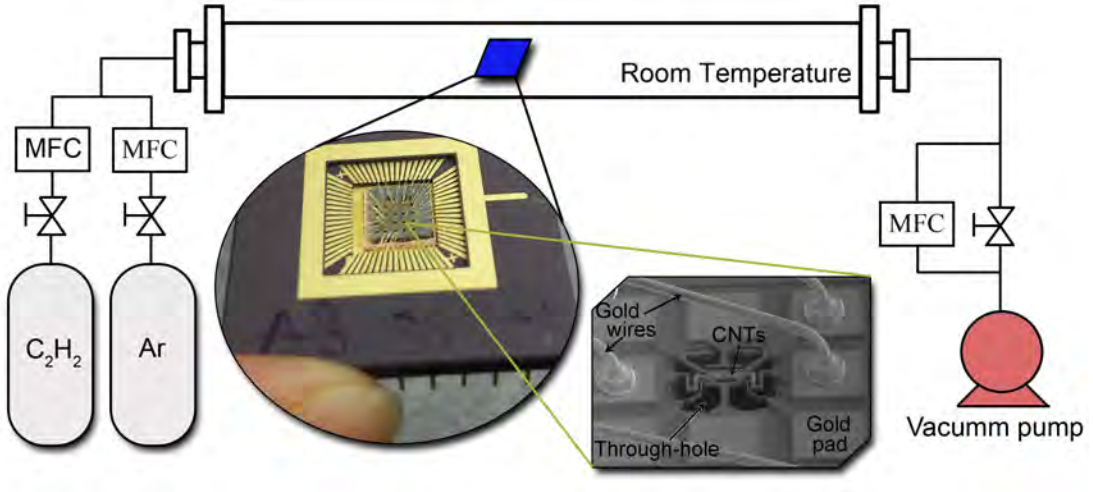

Figure 3.5: Experimental setup for the local synthesis and direct integration of CNTs into a microsystem. The vacuum chamber has an electrical feedthough. C_2H_2 and Argon are connected to the chamber through mass flow controllers (MFCs).

Figure 3.7 shows a resulting Si/CNTs/Si microsystem after the synthesis process. The CNTs are suspended and span the two Si microelectrodes. The number of CNTs that span two microelectrodes can be *in-situ* monitored during the synthesis through measurements of the electric current passing the Si/CNTs/Si system (indicated by the amperemeter (A) in Figure 3.6). When a CNT connection was established, a step-increase in the electric current occurred. Conversely, the loss of a CNT connection leads to a step-decrease in the electric current. Each CNT connection might involve in one or more CNTs connecting the two microelectrodes within the measurement delay time ($\sim$1 second). Figure 3.8 shows the *in-situ* monitoring of CNT connections during a synthesis. In this experiment, the first step-increase occurred around 50 seconds after C_2H_2 gas flow was initiated. Twenty-five seconds later, the

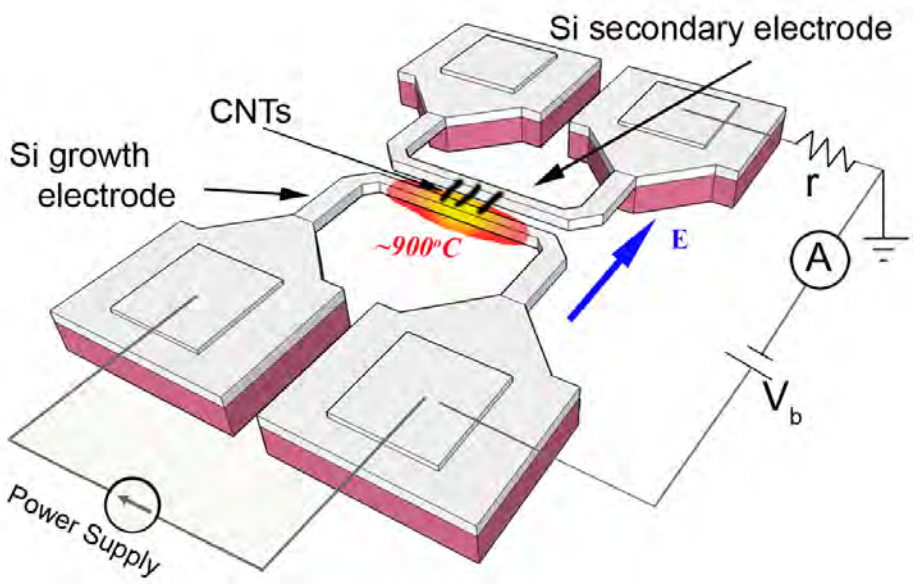

Figure 3.6: Circuitry for the local synthesis and direct integration of CNTs into a Si microsystem. Electrical signals are supplied and/or measured through a Keithley 2602 Dual channel. The Keithley and MFCs are controlled through a LabView program. The resistor (r) is optionally used to limit the current going through the Si/CNTs/Si system.

first CNT connection was lost. A loss of CNT connection might be due to losing the contact between CNT and Si microelectrodes, or due to breaking of CNTs. After 10 more seconds, a new connection was established, but lost after several seconds. After ∼20 more seconds, a new connection was established, and so on.

A key contribution of this thesis is a simple and robust method to control the temperature for the growth of CNTs by using only *in-situ* measurements of the electrical resistance of the Si microelectrode. Details about the method described above is presented in *Article P1*. The principle is briefly explained as follows. In the following, T is referred to as the temperature at the center of the growth electrode induced by Joule heating, and R is referred to as the electrical resistance of this electrode. Since the resistivity of Si (doped) is highly sensitive to the temperature, R is thus strongly correlated with T. The input electrical power (P) is correlated with the induced temperature, and thus being correlated with R. This P-R relationship has the following characteristics:

(i) at a low P: T is also low, an increase in P leads to an increase in T, which leads to a decrease in the mobility of charge carriers (due to phonon scattering), then leads to an increase in R.

(ii) at high P: T is also high, then an increase in P leads to an increase in the number of charge carriers, dominating the scattering effect, thus leads to a decrease in R.

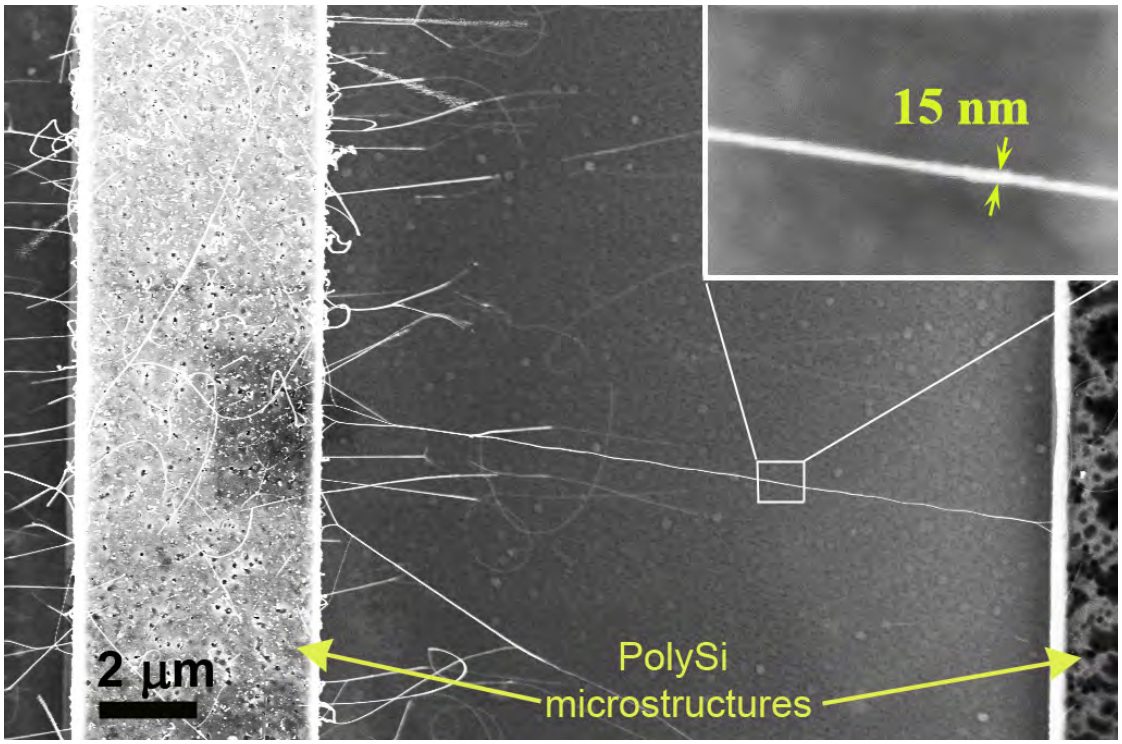

Figure 3.7: SE-SEM micrograph of a PolyMUMPs microsystem after the synthesis process. A CNT is suspended and span the two Si microelectrodes.

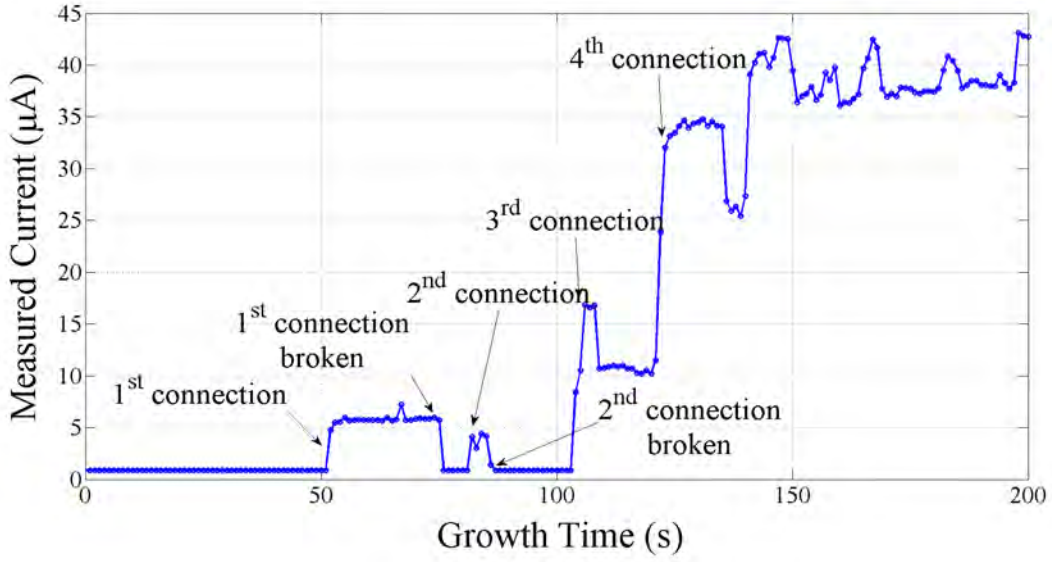

Figure 3.8: *In-situ* monitor of the CNT connections through measurements of the electric current passing the Si/CNTs/Si system. Each step-increase (or decrease) is corresponding to an establishment (or a loss) of a CNT connection.

By means of experimental calibrations (using temperature-indicating paints), a *P-R-T* relationship was obtained, as shown in Figure 3.9. This relationship is as follows: T will be 700-750°C when R reaches maximum; T will be 800-850°C when R falls down ∼5% after the maximum point; and T will be 900-950°C when R falls down ∼10% after the maximum. Note that the exact value of the heating power varied from sample to sample, however, the evolution as shown was similar for all samples. This *P-R-T* relationship could thus be applied to all synthesis experiments.

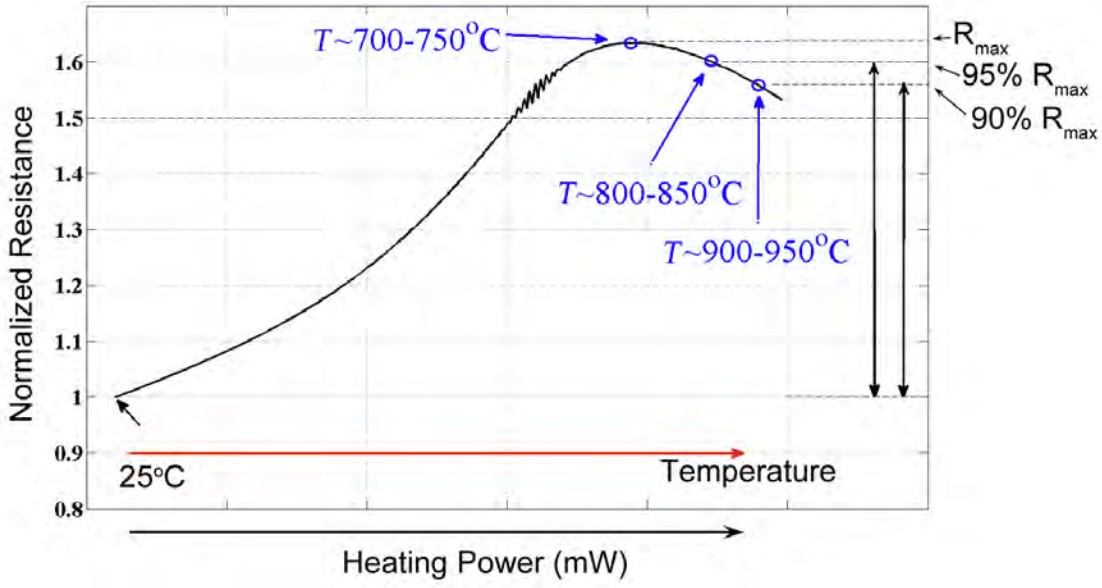

Figure 3.9: The *P-R-T* relationship, between the input power for heating the growth electrode (*P*) and the electrical resistance of the electrode (*R*), together with several data points of the induced temperature at the center of the electrode (*T*). Normalized resistance is defined as the ratio *R(P)/Ro* where *Ro* is the initial resistance before heating. The exact value of *P* varied from sample to sample, however, the evolution of *R* upon increasing *P* was similar for all samples.

Using the *P-R-T* relationship, we can control the synthesis temperature by using only electrical signals. The number of CNT connections is also monitored through electrical signals only, as mentioned earlier. Accordingly, the entire synthesis and integration process is electrically controlled. Pure electrical control has following advantages: (i) simple and robust, and (ii) enable a simple, automated and parallel synthesis and integration of CNTs into Si microsystems.

Chapter 4

Effect of Synthesis Conditions on the Characteristics of CNTs

4.1 Effect of temperature on diameter and density of CNTs

The distribution of CNTs along the growth electrode was found to be non-uniform. This is a result of the temperature gradient created by Joule heating, as shown in Figure 4.1. Detailed results and discussions are presented in *Article P4*. Briefly described, the density of CNTs at the center of the growth electrode (where the temperature was $\sim$900°C) was $\sim$1 μm^{-2}. This region is referred to as *Region D* in the article. Away from the center, the density of CNTs increased, reaching a maximum value of $\sim$57 μm^{-2} at half way to the end of the growth region (referred to as *Region B*). At the end of the growth region where the temperature was $\sim$800°C (referred to as *Region A*), the density decreased to $\sim$50 μm^{-2}. The average diameter of CNTs at *Region D* was 8.0 nm, and increased to 10.8 nm at *Region B*, and continued to increase to 13.7 nm at *Region A*.

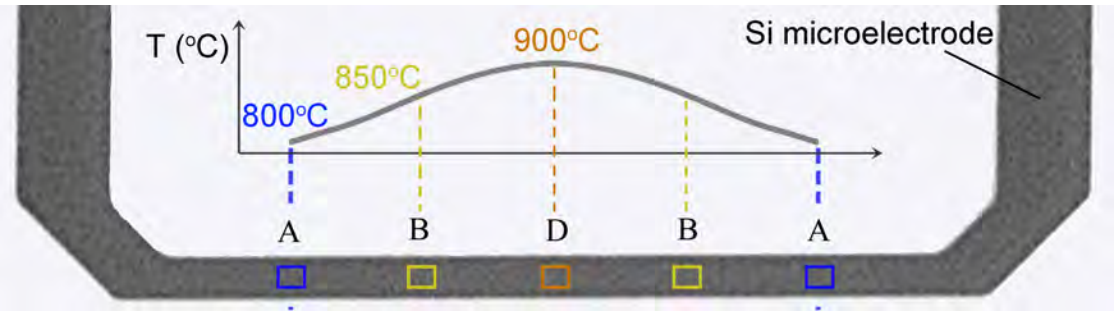

Figure 4.1: Simulated temperature profile on the growth microelectrode resulting from Joule heating (a finite element simulation).

4.2 Effect of temperature on the growth structure of CNTs

The temperature gradient along the growth electrode allows for studying the effect of temperature on the resulting CNT structure. A correlation between the local temperature and the structure of CNTs was revealed: the higher the growth temperature, the higher the degree of order in the CNT structure. Most regular CNTs were found at the center of the microelectrode where the temperature is highest ($\sim$900^{o}C). At the lowest-temperature region ($\sim$800^{o}C), CNTs were found with the highest degree of disorder and defect, such as bamboo-like CNTs or even carbon fibers. At the intermediate-temperature region ($\sim$850^{o}C), CNTs were found with a moderate degree of disorder: fairly uniform diameter, but have several broken and bent sites along the CNT length. Detailed results are reported in *Article P3*.

4.3 Effect of the electric field on the growth orientation of CNTs

4.3.1 The overall picture

The electric-field-assisted growth and alignment of CNTs have been well documented in literature [157–160]. This thesis also shows that the electric field affects the growth orientation of CNTs. Figure 4.2 presents some examples of CNTs being well-aligned with the electric field. It is, however, important to note that not all CNTs are aligned with the electric field direction; and the next section will explain.

4.3.2 Diameter dependency for the electric-field-assisted growth of CNTs

A statistical analysis of 1100 CNTs revealed the diameter dependency of the effect of an applied electric field on the growth orientation of CNTs: small-diameter CNTs (d < 5 nm) are mostly straight and aligned with the electric field; whereas the large-diameter CNTs (d > 10 nm) are curved and do not align with the field. In the transition regime, CNTs were moderately curved, but their average orientation was at small angle with the electric field direction. The overview picture of this finding is shown in Figure 4.3. Detailed results are presented in *Article P2*.

Note on the effect of gas flow:

In the experiments presented above, the gas flow was parallel to the electric field direction. It raised a concern that the gas flow might affect the growth orientation of CNTs. However, by means of the following experiments, it was confirmed that the gas flow did not have an effect:

(i) Experiments with arranging the gas flow perpendicular to the electric field direction, while keeping similar synthesis conditions as in the experiments presented in *Article P2*.

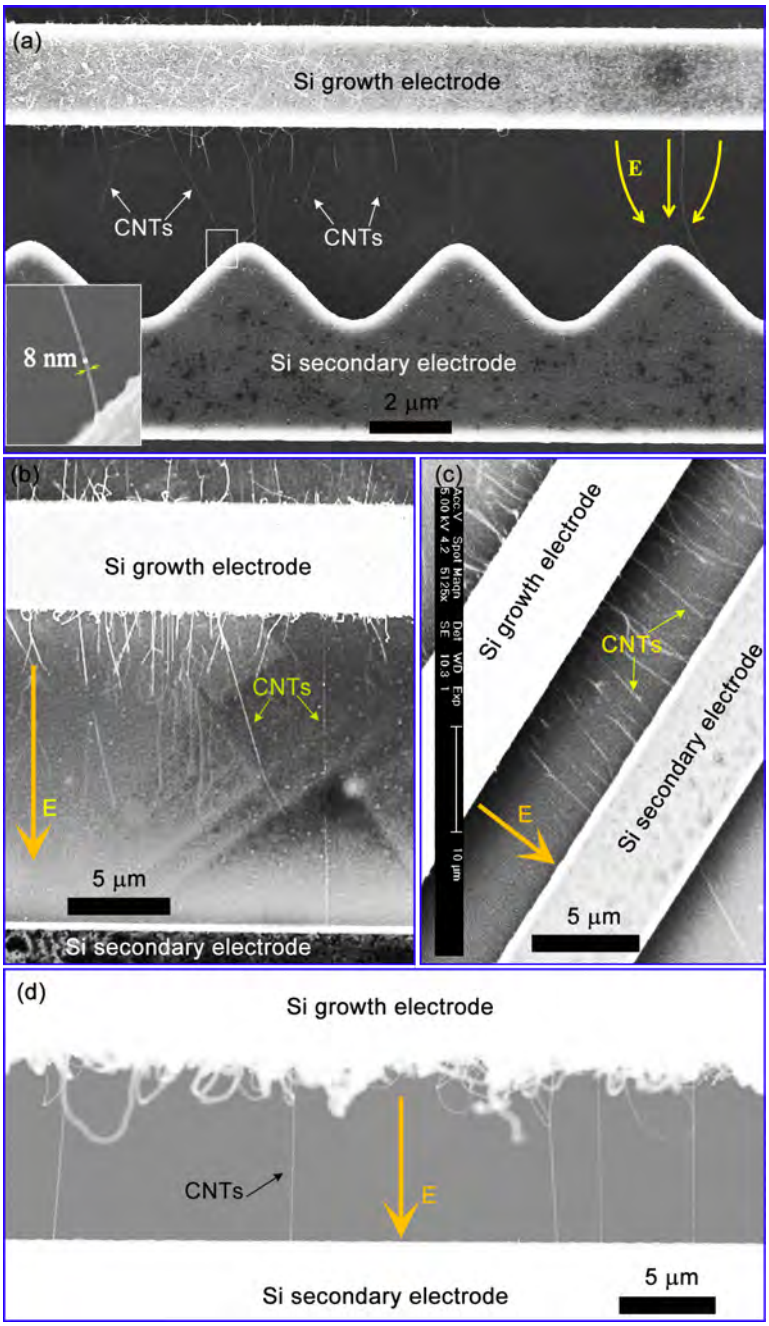

Figure 4.2: SE-SEM images showing many CNTs are aligned with the direction of the applied electric field. (a) The electric field would concentrate at the pointing tips of the secondary microelectrode, the CNTs appear to "concentrate" at pointing tips as well. (b-d) CNTs connecting the two microelectrodes are well-aligned with the direction of the applied electric field. Images (a-c) were taken by the SEM Philips XL30 at 5 kV; image (d) was taken by the Hitachi S-5500 at 30 kV.

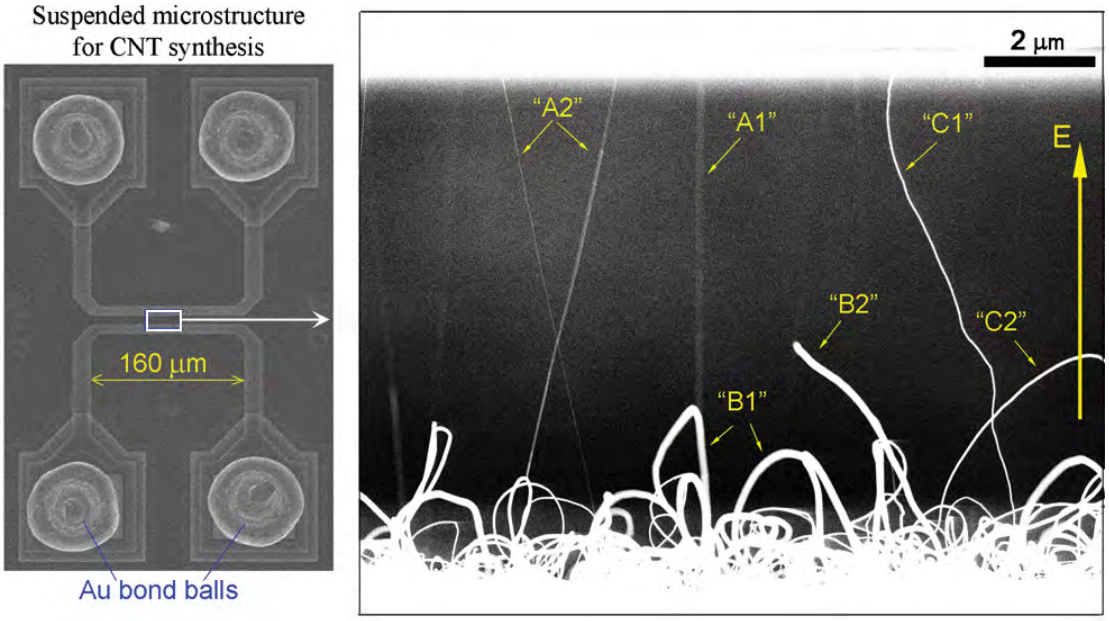

Figure 4.3: The diameter-dependency for the effect of the electric field on the growth orientation of CNTs. The CNTs were grown locally and integrated directly into a microsystem of two suspended Si microelectrodes. ("A") Small-diameter CNTs appear to be straight and well-aligned with the direction of an applied electric field; whereas ("B") large-diameter CNTs are curved and do not align; ("C") Transition regime: CNTs were moderately curved, but their average orientation was at small angle with the electric field. The electric field strength $E =\sim 1.5\ V/\mu$m.

(ii) Experiments with almost zero gas flow rate, while keeping similar synthesis conditions as in the experiments presented in *Article P2*. The gas mixture (C_2H_2 + Ar) were introduced into the chamber only for about 20-30 seconds at the beginning.

In all experiments, the orientation of CNTs were observed to be independent on the gas flow configurations. Note that the gas flow rates used in all experiments were 50 ccm for both Argon and C_2H_2. Different experimental setups may result in totally different outcomes, for example, Huang et al. demonstrated a technique that uses the gas flow to assist the growth orientation of CNTs [161].

Chapter 5

Electrical Characterizations of Si/CNTs/Si systems

5.1 CNT-Si contact modes

There are three possible modes of contact between a Si microelectrode and a CNT. Figure 5.1 illustrates these three contact modes:

Mode (i): CNT-Si tip contact, i.e. the CNT makes contact with the Si electrode by its tip only.

Mode (ii): Si-CNT side contact, i.e. the CNT makes contact with the Si electrode by lying on the electrode.

Mode (iii): Si-$Fe_{particle}$-CNT contact, i.e. the CNTs connects with the Si electrode through a Fe nanoparticle.

At the growth electrode, if the CNT grows in the root-growth mode (i.e. the CNT grows on an Fe particle that stays on the substrate), a contact of *mode (iii)* will be created. Otherwise, if the CNT grows in the tip-growth mode (i.e. the CNT grows underneath the Fe particle that is lifted away from the substrate), a contact of *mode (i)* or *mode (ii)* will be created.

At the secondary electrode, if the CNT grows in the root-growth mode, a contact of *mode (i)* or *mode (ii)* will be created; otherwise, a contact of *mode (iii)* or a combine of *mode (iii) and (ii)* will be created.

Detailed observations on the contact modes between CNTs and Si microelectrodes are presented in *Article P4*.

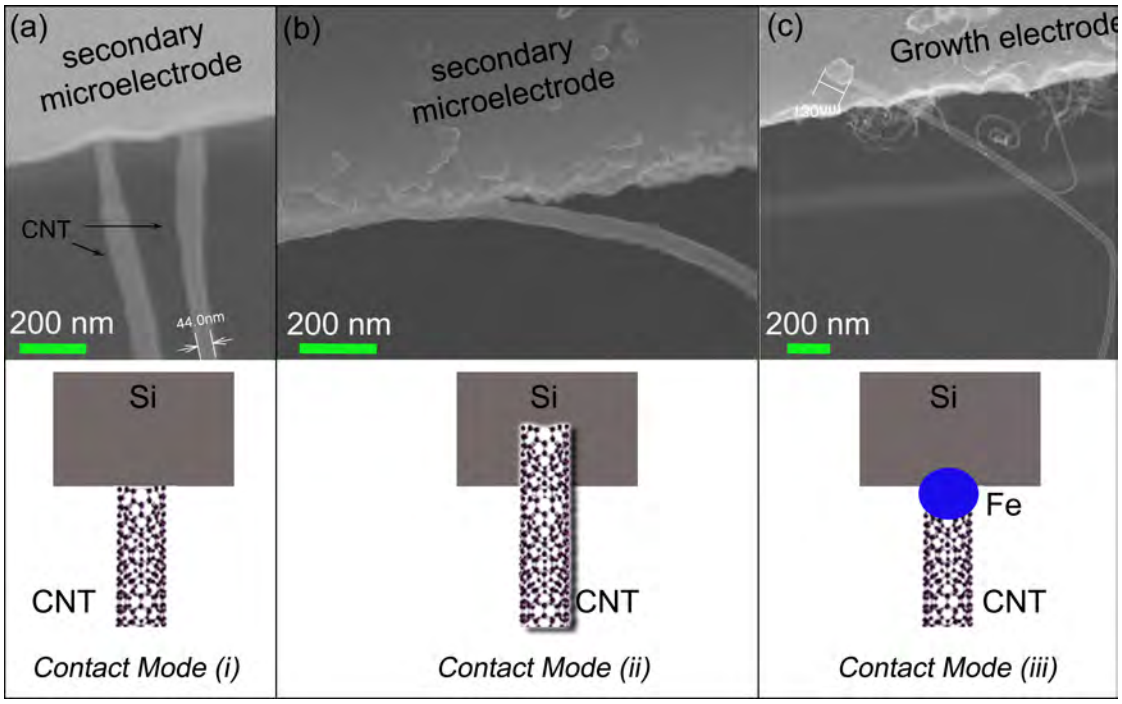

Figure 5.1: Contact modes between a CNT and a Si microelectrode in a Si/CNTs/Si system. (a) *Mode (i)*: Si-CNT tip contact. This type of contact is formed when a CNT attaches to the Si electrode by the CNT tip. (b) *Mode (ii)* Si-CNT side contact. This type of contact is formed when a CNT lies on the Si electrode. (c) *Mode (iii)*: Si-Fe$_{particle}$-CNT contact. This type of contact is formed when a CNT connects with the Si electrode through a Fe nanoparticle.

5.2 Electrical properties of Si/CNTs/Si systems

Current (I)-Voltage (V) measurements were carried out to study the electrical properties of the fabricated Si/CNTs/Si systems. The measurements were taken between the two Si electrodes, as depicted in Figure 5.2. The measured resistance consists of both the intrinsic resistance of the CNTs, and the contact resistance at the CNT-Si interfaces. The current data were insufficient to distinguish these resistances. The intrinsic resistance of the CNTs could be realized by using a nano-probing system, however, it is extremely challenging to probe all individual CNTs in a Si/CNTs/Si system without breaking them or altering their electronic properties. At the current stage, each Si/CNTs/Si systems was characterized as a whole.

At a later stage, an attempt to distinguish the intrinsic resistance of CNTs and the contact resistance was conducted. All CNT-Si contacts in a Si/CNTs/Si system were locally covered with Platinum (Pt) by using the local deposition function of the FEI Helios NanoLab Dual-Beam FIB at NTNU NanoLab, Norway. The deposition of Pt could be localized at a spot size of $\sim$300 nm $\times$ 300 nm. Preliminary experiments showed that the electrical behavior of a Si/CNTs/Si system, which was initially Schottky diode-like, became near-ohmic after the local deposition of Pt at all the contacts. This suggests that CNT-Si contacts may play an important role in the electrical behavior of a Si/CNTs/Si system. Chapter 6, section 6.2.2 will present this preliminary result.

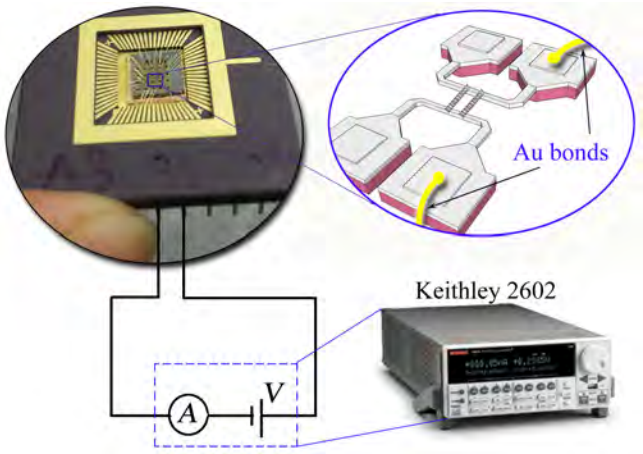

Figure 5.2: *I-V* measurements of a Si/CNTs/Si system were taken between the two Si electrodes. The Keithley 2602 swept the source voltage and measured the current.

5.2.1 PolyMUMPs Si/CNTs/Si systems

Figure 5.3 shows the *I-V* measurements of selected PolyMUMPs Si/CNTs/Si systems. The bias voltage was swept from -1 V to +1 V. Data for larger voltage values were not recorded, since it could break the CNT connections. The values of the current (I) were averaged for one CNT connection, by taking the measured values divided by the number of CNT connections recorded during synthesis. Note that each CNT connection is associated with one or more than one CNT that connect the two Si electrodes within the measurement delay time ($\sim$1 s).

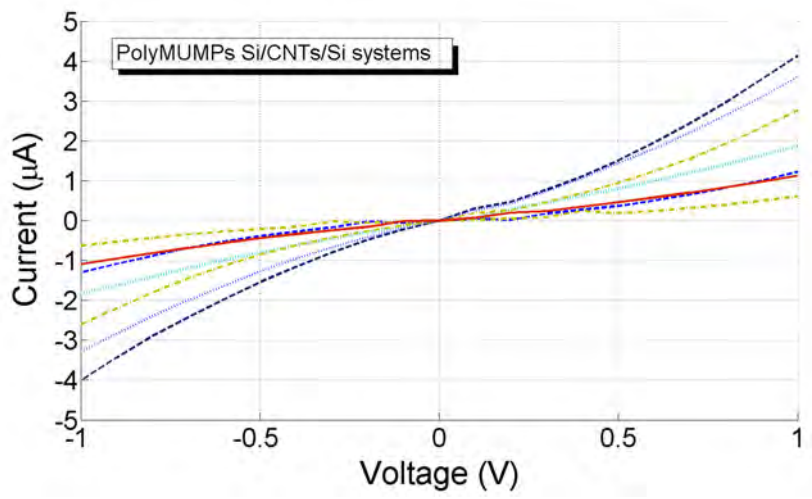

Figure 5.3: *I-V* curves of selected Si/CNTs/Si systems (with polysilicon microelectrodes). The obtained I-V curves are fairly linear, indicating a fairly ohmic behavior of the CNT-polysilicon contact.

The exact number of CNTs could be determined by using a high-resolution SEM, however, it requires a huge labor work to count all the CNTs. Moreover, my access to a high-solution SEM was limited.

The obtained *I-V* curves were fairly linear, indicating the near-ohmic behavior of the CNT-polysilicon contacts. The overall resistances of the selected Si/CNT/Si systems were in the range 250-2000 kΩ. The overall resistance is defined as the inverse of the slope of the straight line connecting two ends of a *I-V* curve.

The intrinsic resistance of a CNT is estimated to be $\sim$ 100 kΩ. The estimate was made as follows. The CNTs in the selected systems had a diameter of 20-40 nm (measured by SEM), thus probably being MWNTs. We have learned from literature (section 2.1.1) that MWNTs with a diameter of 9 nm are diffusive conductors with a well-defined resistance per unit length ($\sim$ 10 kΩ/μm), and that the larger the diameter of a CNT, the more metallic the electrical behavior of the CNT. Each CNT in the selected systems had a length of $\sim$10 μm, and thereby would have an intrinsic resistance of less than 100 kΩ, or 10^5 Ω.

The contact resistance at a CNT-Si interface is estimated to be 10^3-10^7 Ω by using the metal-silicon junction model (discussed in section 2.1.2). The following information was used for the estimation: CNT diameter is $\sim$30 nm, polysilicon is n-doped with a concentration of 10^{19}-10^{20} cm^{-3}. Table 5.1 summerizes the measured and estimated resistances that are mentioned above. The data suggest that the contact resistance at the CNT-Si interface could dominate the total resistance of a Si/CNT/Si system.

Note that the estimates were made with an assumption that the CNT structure is almost perfect. One can see that the CNTs produced in this thesis were often defective (shown in *Article P3*, and *P4*). However, note that the highly defective CNTs, such as bamboo-like CNTs and helically coiled CNTs, did not span the two Si electrodes. Only the CNTs that span two Si electrodes were included in the measured resistance of a Si/CNTs/Si system;

Table 5.1: Measured resistance of a Si/CNT/Si system, and estimated resistance of a CNT and a CNT-Si contact.

	Si/CNT/Si system	Intrinsic CNT	CNT-Si interface
Measured resistance	2.5×10^5 - 2×10^6 Ω	N/A	N/A
Estimated resistance		$<10^5$ Ω	10^3-10^7 Ω

N/A - Not Available.

and these CNTs were mostly straight and had few defects. Therefore, the above estimates are still be reasonable.

5.2.2 SOIMUMPs Si/CNTs/Si systems

Both near-ohmic and non-ohmic *I-V* curves were observed in SOIMUMPs Si/CNTs/Si systems. Figure 5.4 shows the *I-V* curves of near-ohmic systems. In fact, a CNT-Si contact would behave as a near-ohmic contact when the Si is heavily doped [77]. The doping concentration of the silicon in SOIMUMPs microsystems is highest at the top surface ($\sim10^{20}$ cm^{-3}), and decreases with distance down into the silicon. This suggests that the CNT-Si contacts in near-ohmic systems were likely to locate at the top surface of the Si electrodes. This scenario is illustrated in Figure 5.7.

Figure 5.5 and Figure 5.6 show the *I-V* curves of systems having rectifying or diode-like behaviors. Some systems exhibited a behavior like one single Schottky diode, as shown in Figure 5.5. Some systems exhibited a behavior like two Schottky diodes in a back-to-back configuration, as shown in Figure 5.6. The breakdown voltages of these non-linear systems were about 2 - 8 V, which is the typical range for the SOIMUMPs Si/CNTs/Si systems.

From the literature presented in Chapter 2, section 2.1.1, we learned that the breakdown voltage of a CNT-Si contact is estimated to be 2 - 8 V when the doping concentration of

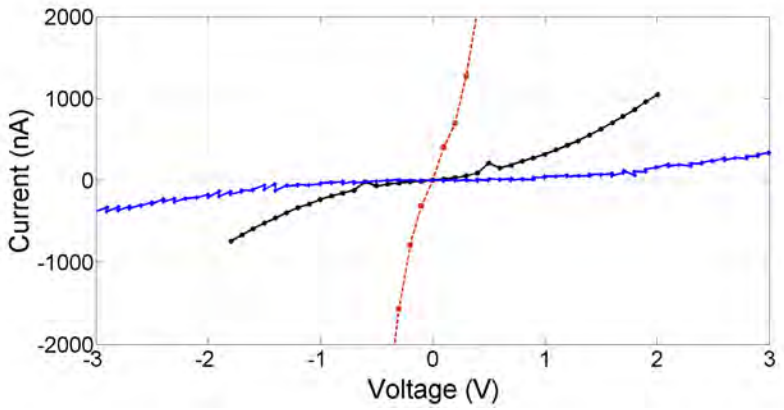

Figure 5.4: Near ohmic *I-V* curves of selected SOIMUMPs Si/CNTs/Si systems.

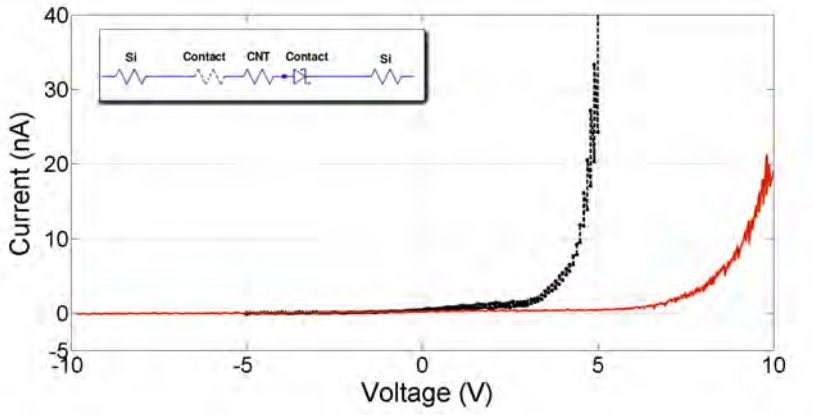

Figure 5.5: *I-V* curves of selected SOIMUMPs Si/CNTs/Si systems that behave like a single Schottky diode. The inset depicts a electrical model for these systems.

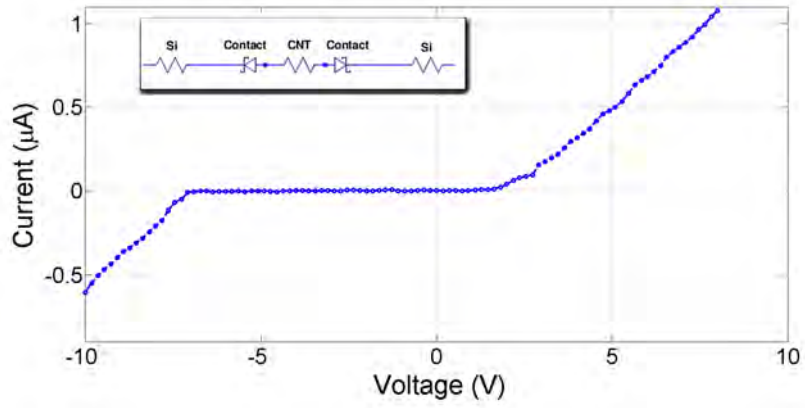

Figure 5.6: *I-V* curve of selected SOIMUMPs Si/CNTs/Si system that behave like two Schottky diodes in a back-to-back configuration. The inset depicts an electrical model for this system. The model was first proposed by Haugen *et al.* [162].

n-type Si is on the order of 10^{18} cm^{-3}. This suggests that the CNTs in the selected systems made contact with the Si electrodes at the positions where the doping concentration of Si is $\sim 10^{18}$ cm^{-3}. Such a position is estimated to be $\sim$500 nm below the surface, as illustrated in Figure 5.7(c). This estimation was made by using Fick's Laws with the model "limited source near the surface", and the following information: in SOIMUMPs, the Si layer was doped by depositing a phosphosilicate glass layer and annealing at 1050^{o}C for 1 hour in Argon.

Details about the electrical properties of SOIMUMPs Si/CNTs/Si systems were reported by Haugen et al. [162] and Haugen's master thesis [156]. I am a co-author of the paper, and a co-supervisor of the master thesis.

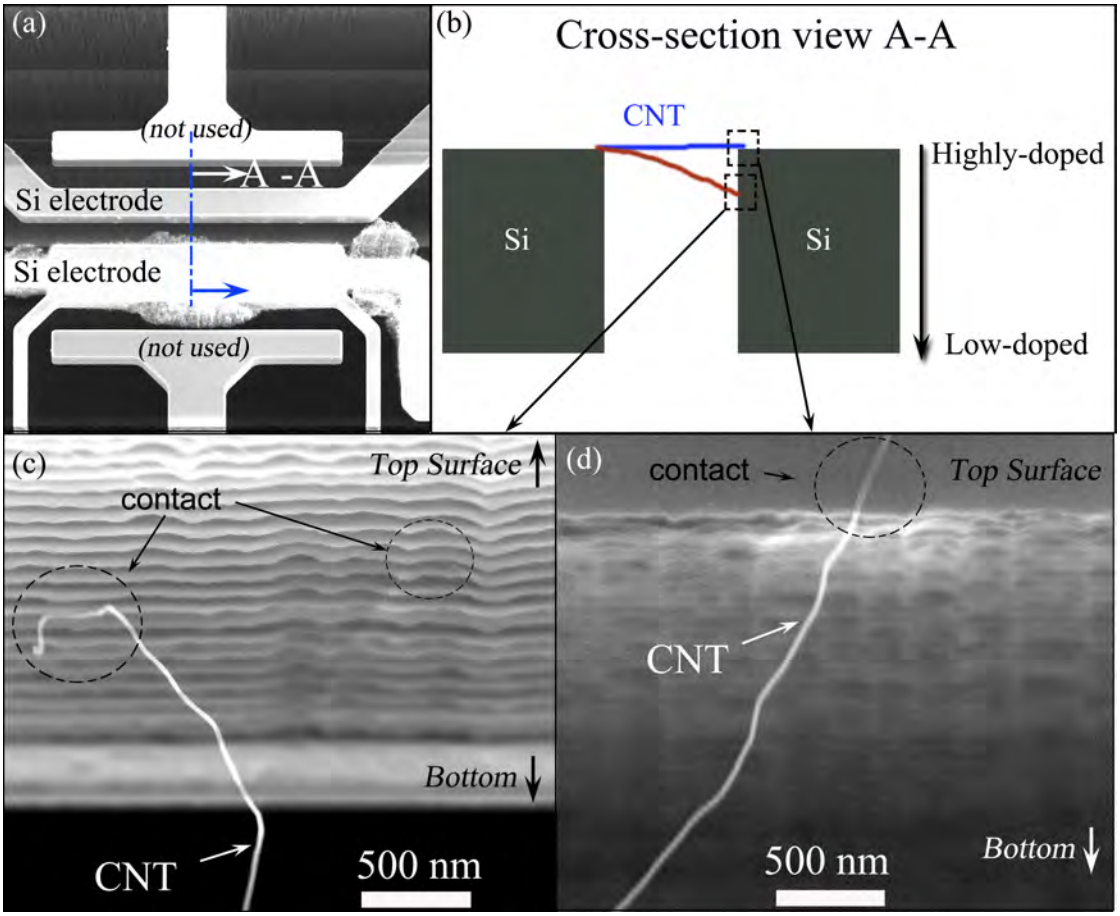

Figure 5.7: Doping concentration varies along the depth of the Si microelectrodes. CNT-Si contacts at different positions of different doping concentration would exhibit different electrical behaviors. (a) Overview of a SOIMUMPs microsystem. (b) Cross-section illustration of different scenarios for a CNT-Si contact. (c) An SE-SEM image showing two CNT-Si contacts at positions below the surface. (d) An SE-SEM image showing a CNT-Si contact at the top surface of a Si microelectrode. Abbreviation: SE = Secondary Electron.

Chapter 6

Sensor Applications and Developments

6.1 Si/CNTs/Si systems as NH_3 sensors

A NH_3 gas sensor using a PolyMUMPs Si/CNTs/Si system is demonstrated. After the synthesis process presented in Chapter 3, the as-fabricated systems were then tested for their sensitivity to NH_3 gas. The sensor experiments were carried out as follows: The chip containing a selected Si/CNTs/Si system was placed in an evacuated chamber with an electrical feedthrough. A voltage bias of 0.1 V was applied between the two Si microelectrodes of the selected system, and the electric current through the system was recorded every second. Figure 6.1 shows a SEM micrograph of the selected Si/CNTs/Si system and the circuitry for the sensor experiment. A known amount of NH_3 was introduced into the chamber. When the response was settled, the chamber was evacuated before exposure to a new amount of NH_3. The effective concentration of NH_3 in the chamber was calculated from the volume of NH_3 gas injected into the chamber. This volume was extracted by a syringe from a closed flask containing NH_3 gas. The amount of NH_3 in the flask is determined by the amount of NH_3/ethanol solution injected into the flask. Figure 6.2 shows the response of the selected Si/CNTs/Si system towards NH_3. The electric current through the system decreased upon exposure to NH_3. For instance, the electric current decreased $\sim$1% upon exposure to NH_3 at a concentration of 442 ppm. The sensor had, however, a low reversibility: the recovery time was greater than 500 seconds.

A simple technique to improve the reversibility of the sensor was found: switching the bias voltage off while evacuating the chamber for the recovery of the sensor; switching the bias voltage on again just before the next exposure. Figure 6.3 shows the response of the same Si/CNTs/Si system that was presented in Figure 6.2. The reversibility of the sensor was improved significantly. The obtained result has been published in *Article P6*.

CNTs in the selected system were probably metallic MWNTs as their diameters were larger than 10 nm. NH_3 groups are electron-donating, thus providing electrons to the CNTs. Accordingly, the electric current through the CNTs would increase upon adsorption (or absorption) of NH_3. Since the current through the selected Si/CNTs/Si system increased upon exposure to NH_3, it is believed that the response resulted from the CNT-Si contacts, not from

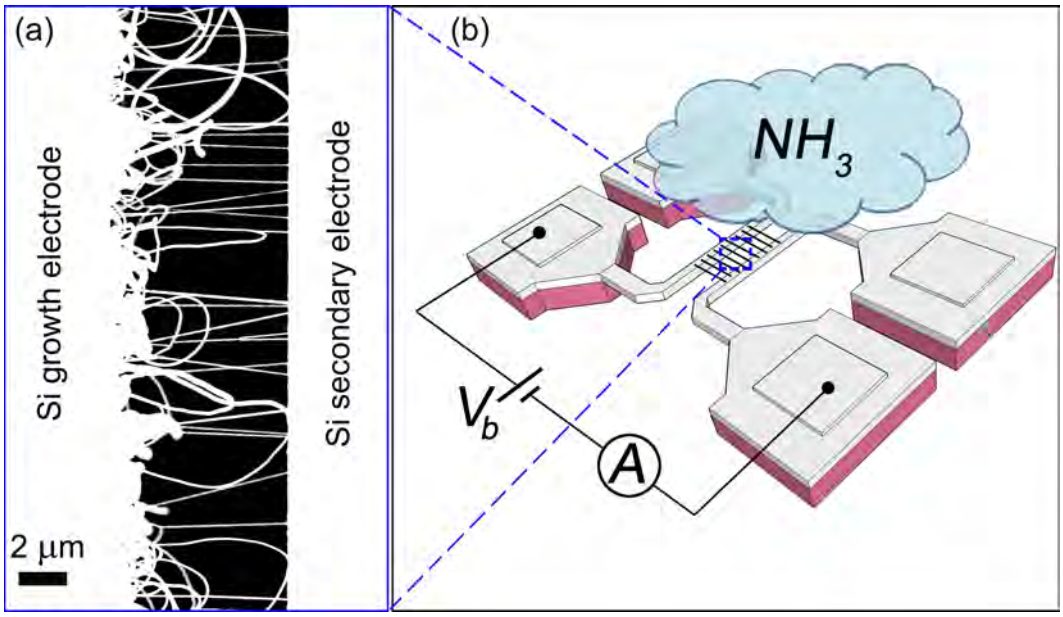

Figure 6.1: Circuitry for NH_3 sensor experiments.

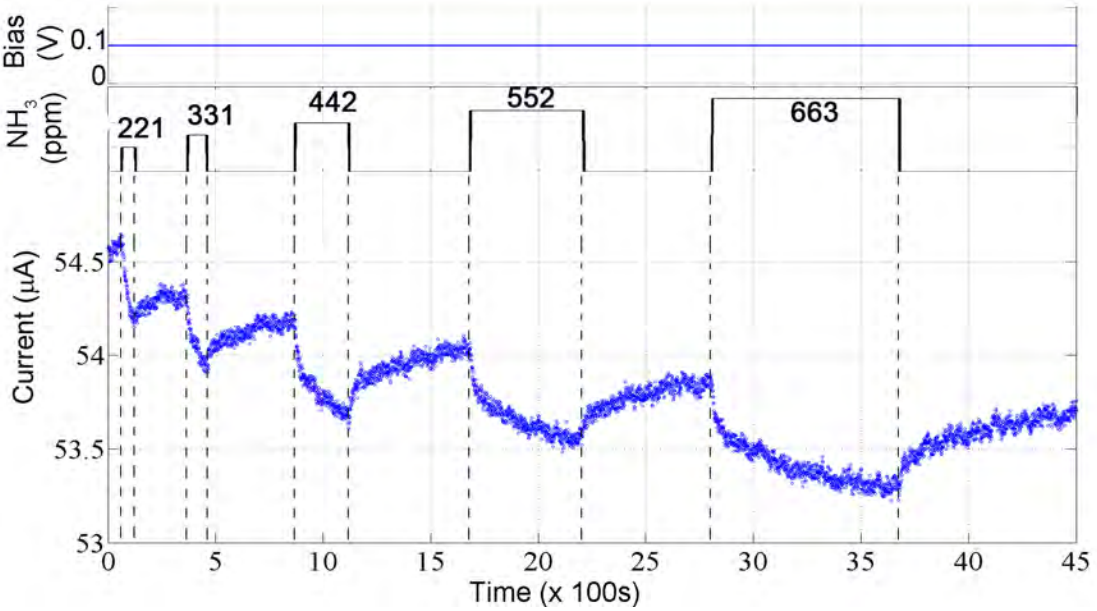

Figure 6.2: Response of a selected Si/CNTs/Si system to NH_3. The chamber was evacuated between successive exposures to NH_3. The bias voltage was kept constant during the experiment.

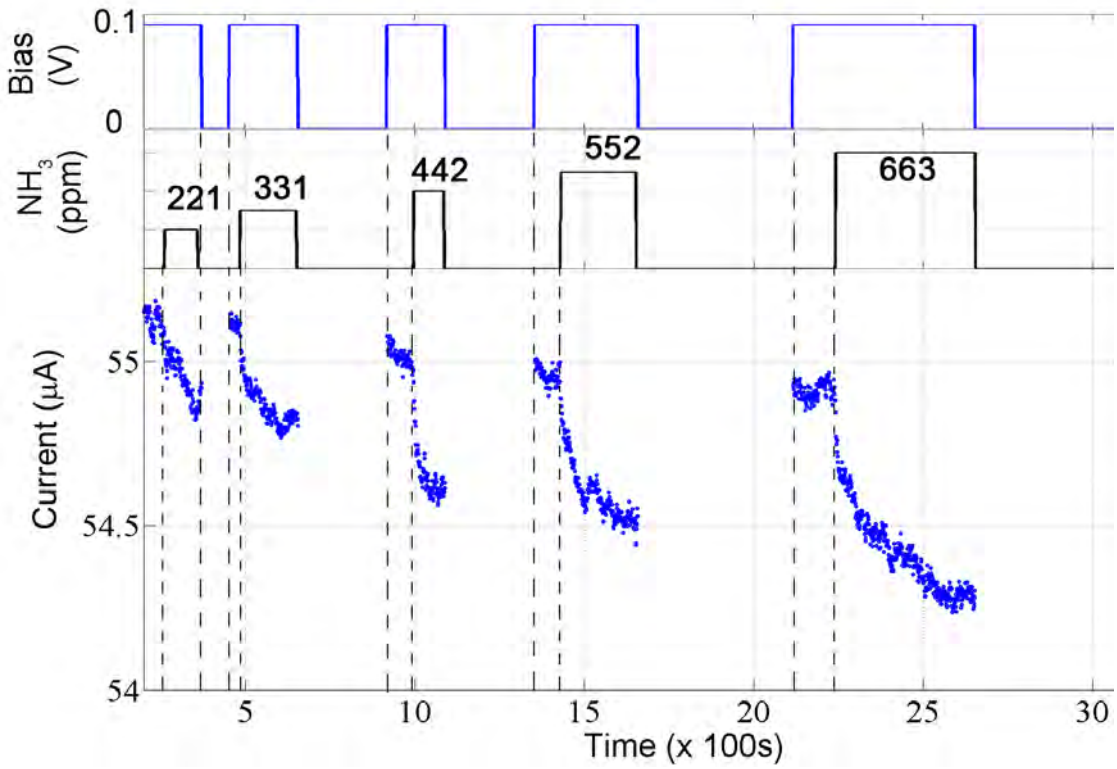

Figure 6.3: Response to NH_3 of the same Si/CNTs/Si system that was presented in Figure 6.2. The bias voltage was switched off during the evacuation periods.

the CNTs. In fact, previous studies in literature have shown that the contacts could play the major role in the sensing performance of a CNT-based sensor. For example, Zhang et al. [163] reported that their metal/CNTs/metal systems became insensitive to NO_2 after the CNT-metal contacts were passivated (by being covered with polymethylmethacrylate). According to Peng *et al.*, the Schottky barrier modulation at the CNT-metal contact dominates the sensing performance of a metal/CNTs/metal system, upon adsorption of NH_3 [164].

6.2 Reducing the contact resistance

As discussed in Chapter 5, section 5.2, the contact resistance at the CNT-Si interface would dominate the overall resistance of a Si/CNTs/Si system. This is unfavorable when using the Si/CNTs/Si system in applications where CNTs are the active element of the system. The CNTs are expected to change their resistance upon absorption (or adsorption) of analytes. The resistance change will not be measurable if it is too small compared to the overall resistance of the Si/CNTs/Si system, since the measurements are taken between the Si electrodes. In another word, high contact resistance at the CNT-Si interface reduces the sensitivity of a Si/CNTs/Si system. Thus, the contact resistance needs to be reduced.

6.2.1 Local annealing of the contact

A simple and fast annealing technique to reduce the CNT-Si contact resistance has been investigated. This work has been conducted in a collaboration with the CNT research group of Professor Liwei Lin at the University of California, Berkeley, USA. The experimental setups are illustrated in Figure 6.4. We implemented two setups. In the 1st setup, an applied electric current goes through the Si/CNTs/Si system. High temperatures at CNT-Si contacts on both Si microelectrodes will be induced by Joule heating, since the CNT-Si contacts have a high resistance. In the 2nd setup, an applied electric current goes through the secondary Si microelectrode and induces high temperatures for annealing the CNT-Si contacts only on this electrode. Only the secondary electrode is chosen because the growth electrode was already heated during the synthesis and thus the CNT-Si contacts on the growth electrode were already annealed.

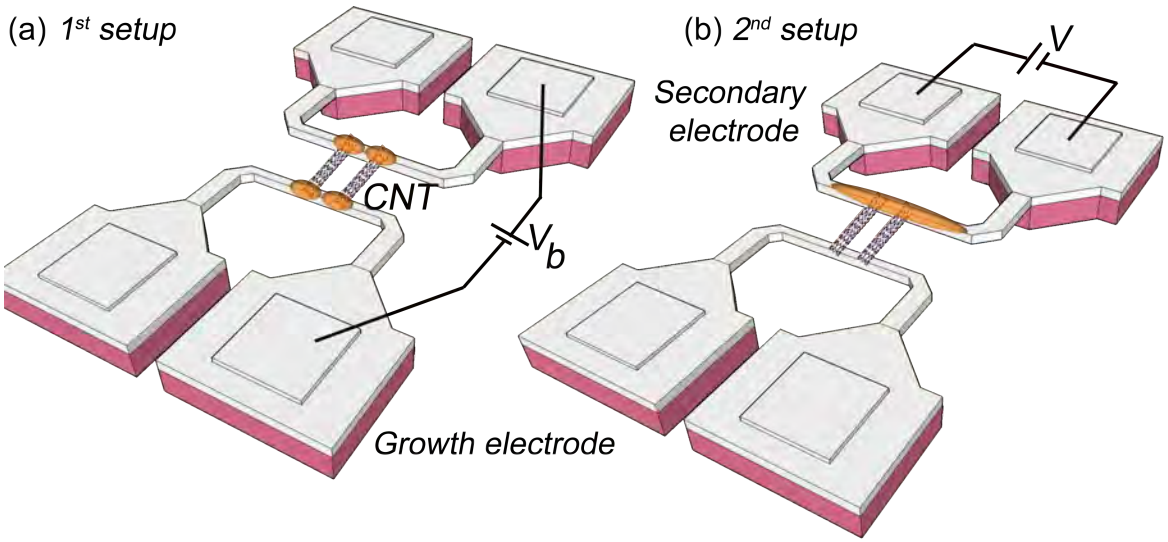

Figure 6.4: Experimental setup for local annealing of CNT-Si contacts to reduce the contact resistance. (a) 1st setup: an applied electric current goes through the Si/CNTs/Si system and induces high temperatures at the CNT-Si contacts on both Si microelectrodes. (b) 2nd setup: an applied electric current goes through the secondary electrode and induces high temperatures to anneal the CNT-Si contacts on this electrode only.

Heather Chiamori et al. [55] reported that this technique reduced the contact resistance for 60% of the samples, and the reduction in resistance ranged from 20% to 80%. The authors also suggested that annealing with a higher power and a longer time would result in more reduction in the contact resistance. I am a co-author of this publication.

In a continued collaboration with Heather Chiamori and Liwei Lin, this thesis has carried out more experiments with high annealing powers, and also carried out the *in-situ* monitor of the annealing process. The resistance reduction was found to be stepwise. Figure 6.5(a) shows the *in-situ* measurement of the resistance of a Si/CNTs/Si system during annealing (using the 2^{nd} setup). The origin of the step changes has not yet been found. The *I-V* curves of the above sample before and after annealing are shown in Figure 6.5(b). The annealed Si/CNTs/Si system appeared to have lower resistance.

More results will be presented in the upcoming publication, being written by Heather Chiamori, Bao Q. Ta, Knut E. Aasmundtveit, and Liwei Lin.

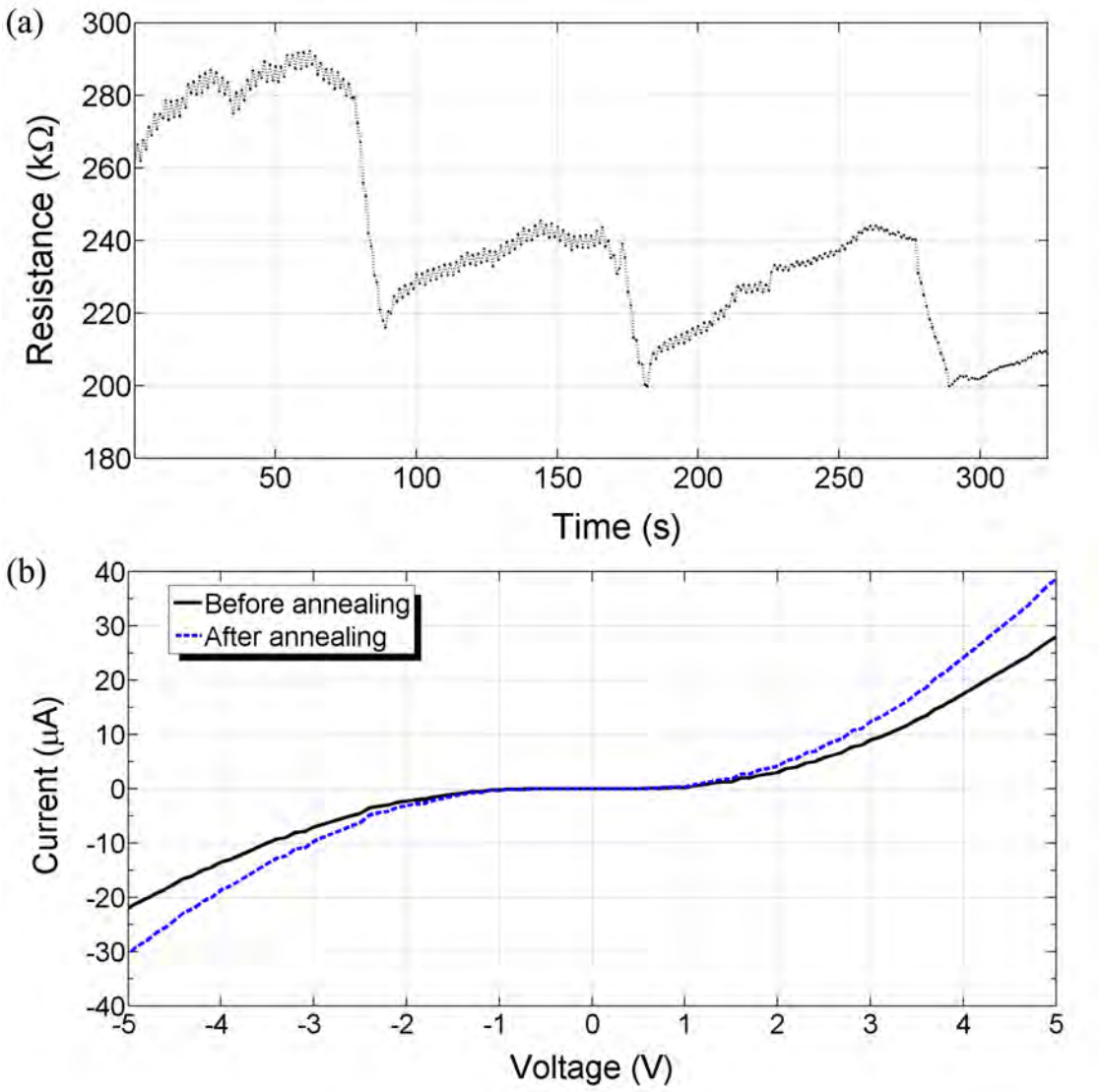

Figure 6.5: (a) *In-situ* monitoring of the resistance of a Si/CNTs/Si system during the annealing process (using the 2^{nd} setup). (b) *I-V* curves of the Si/CNTs/Si system before and after annealing.

6.2.2 Metal deposition at the CNT-Si contact via FIB

The first motivation for this work is to investigate whether the electrical properties of a CNT-Si contact could be improved by locally depositing Platinum (Pt) at the contact. The second motivation is to distinguish the contact resistance and the intrinsic resistance of CNTs. The local deposition of Pt at the CNT-Si contacts were done by using the metal deposition function of the FEI Helios NanoLab DualBeam FIB at the NTNU NanoLab, Norway. The electron beam was used in the deposition process. The deposition of Pt could be localized at a spot size of $\sim$300 nm $\times$ 300 nm, as shown in Figure 6.6.

Since the local deposition process for all CNT-Si contacts in a Si/CNTs/Si system required a lot of labor work and my access to the equipment was limited, only a few experiments have been done. Four Si/CNTs/Si systems have been studied, but three of them were broken after the deposition process. The resulting electrical properties of these three systems were undetermined. The other system clearly showed a significant change in its electrical properties. Before Pt deposition, this Si/CNTs/Si system exhibited a rectifying behavior, with a breakdown voltage of 4 V. After Pt deposition at all CNT-Si contacts, the system exhibited a near-ohmic behavior. This interesting preliminary result suggests that there is a need for further studies.

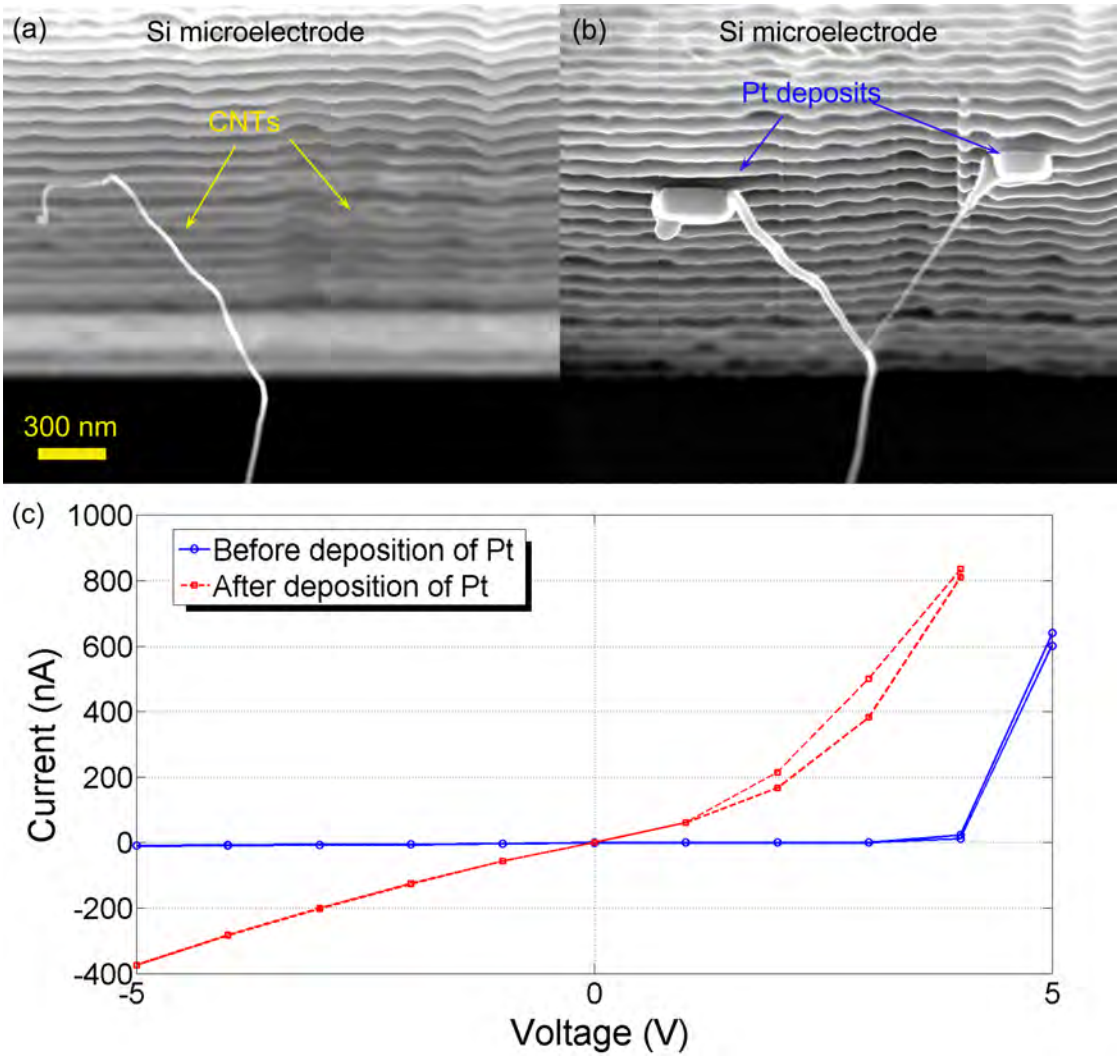

Figure 6.6: SE-SEM micrographs showing two CNT-Si contacts before (a) and after (b) the local deposition of Pt. (c) *I-V* curves of a Si/CNTs/Si system before and after the Pt deposition. For each *I-V* measurement, the voltage swept from 0 V to +5 V and backward to -5 V and then to 0 V to finish a measurement.

6.3 Functionalization of CNTs by thermal evaporation of Palladium and Tin

Previous studies in literature have shown that functionalized CNTs with metal nanoparticles have a better sensitivity and selectivity than pristine CNTs [165, 166]. Star *et al.* [119] have shown great potential of functionalized CNTs with 18 metals/metal oxides (Mg, Al, Ti, V, Cr, Mn, Fe, Co, Ni, Zn, Mo, Rh, Pd, Sn, W, Pt, Au and Pb) for sensor applications. Common techniques for functionalizing CNTs are involved in photolithography, lift-off, solution treatment and sonication [88, 119]. Such processes, however, would destroy the CNTs in a Si/CNTs/Si system where CNTs are suspended and span two Si electrodes. Alternative techniques for functionalizing the suspended CNTs are electron-beam and thermal evaporation. Zhang et al [167] have used electron-beam evaporation to coat Au, Pd, Fe, Al, and Pb on suspended SWNTs. This thesis attempted to use thermal evaporation to functionalize the CNTs in Si/CNTs/Si systems. Palladium (Pd) was first chosen for an investigation. Functionalized CNTs with Pd nanoparticles attached to the CNT surface were produced, as an example shown in Figure 6.7. Detailed results are presented in *Article P5*.

Thermal evaporation of Tin (Sn) on the locally grown CNTs was also investigated. This work was conducted in a collaboration with a master project under my co-supervision [168]. Figure 6.8 shows the resulting CNTs with nanoparticles deposited on the CNT surface. Note that the nanoparticles were probably in form of Tin oxide, due to the oxidation in air during handling of samples. The target thickness of the deposition was 1.6 nm, as similar as for Pd deposition. The resulting Tin oxide nanoparticles were $\sim$2 times larger than the Pd nanoparticles, but the density of Tin oxide nanoparticles was about a half of the density of Pd particles. The size difference could result from the oxidation of Sn particles, whereas Pd particles were not oxidized. The density difference could result from the difference in interaction, nucleation and diffusion rate of metal atoms on CNTs.

The resulting profile of Pd (and Sn) nanoparticles on CNTs are similar to the results of previous studies in literature [113, 165, 166], despite that the functionalization methods are different. Assuming that the sensing mechanism of Pd-CNTs (and Sn-CNTs) is identical, the resulting Si/CNTs/Si systems can also detect H_2, CO, O_2, CH_3CH_2OH (ethanol) and C_2H_4 (ethylene) gases as the CNT-based devices in the previous studies. Since the sensor performance has not yet been tested, the present results are just preliminary results that suggests a potential of using thermal evaporation of Pd (and Sn) to functionalize the CNTs in a Si/CNTs/Si system where CNTs are suspended and span two microelectrodes.

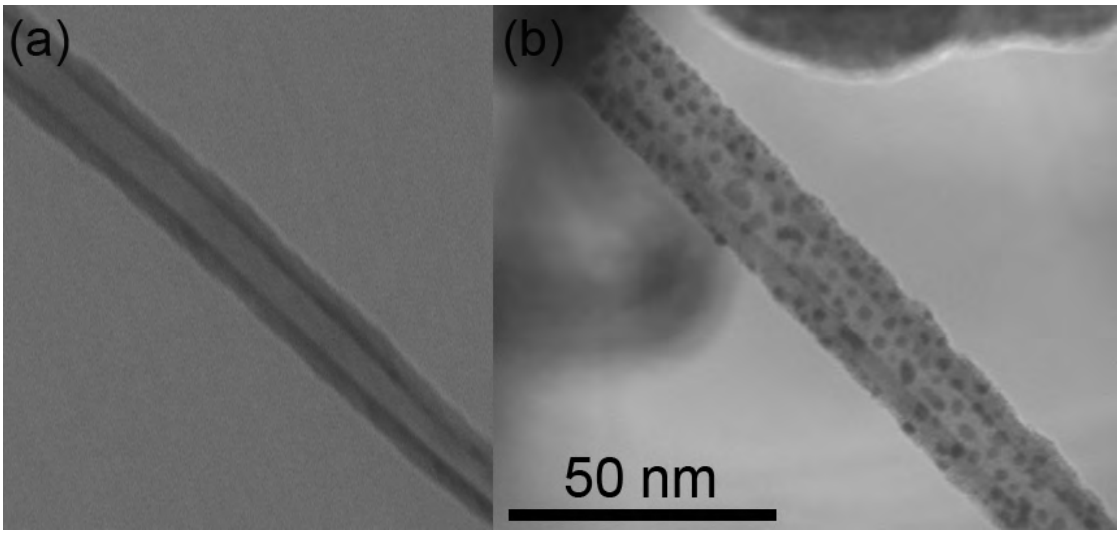

Figure 6.7: Deposition of Pd nanoparticles onto a locally grown CNT, by using thermal evaporation of Pd with a target thickness of 1.6 nm. (Left) Before deposition. (Right) After deposition.

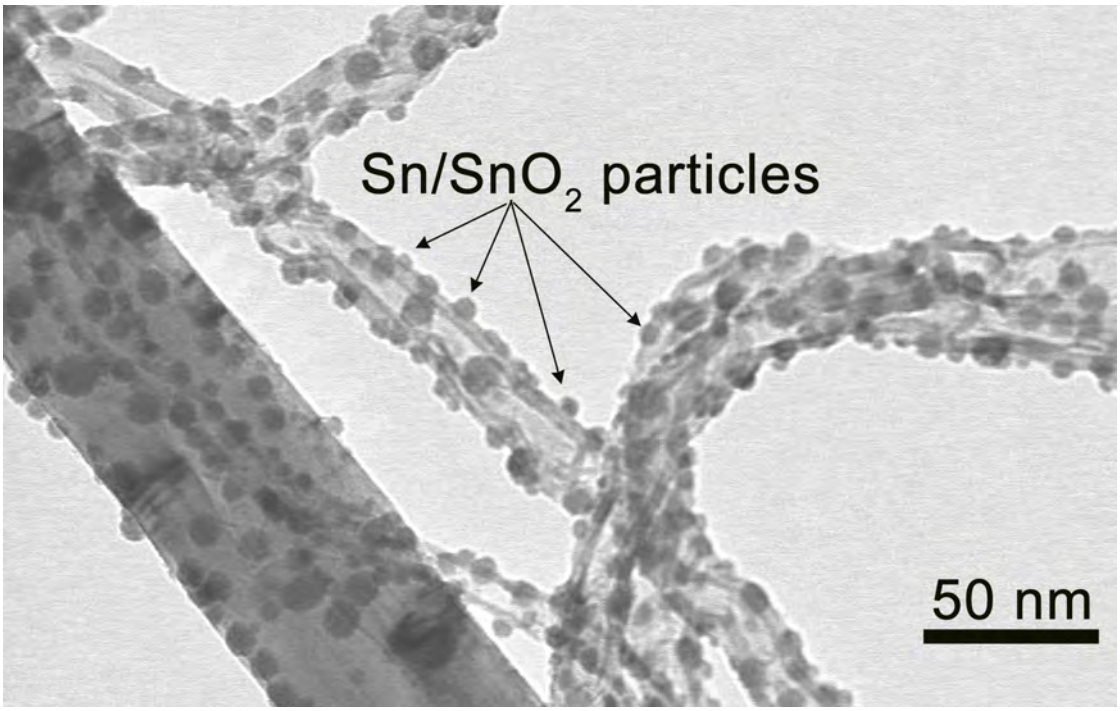

Figure 6.8: Deposition of Tin/Tin oxide nanoparticles onto the locally grown CNTs, by using thermal evaporation of Tin with a target thickness of 1.6 nm. The nanoparticles were probably in form of Tin oxide, due to oxidation in air.

Chapter 7

Conclusion

This thesis has achieved the main goal, which is to develop a single-step, scalable up to wafer-level, well-controlled process for the local synthesis and direct integration of CNTs into Si microsystems. This thesis has also made significant contributions to the fundamental understanding of the CNT growth.

Key contributions of this thesis are summarized as follows:

1. Developed a method of pure electrical control of the synthesis conditions. This method has the following advantages: (i) simple and robust, and (ii) enable a simple, automated and parallel synthesis and integration of CNTs into Si microsystems. The as-fabricated Si/CNTs/Si systems were demonstrated to be working as a NH_3 sensor.

2. Revealed the effect of local temperature on the resulting characteristics of CNTs (diameter, density and nanostructure). The obtained results are useful for designing the microsystems and choosing appropriate temperature to produce CNTs with desired characteristics.

3. Discovered the diameter dependency for the effect of an applied electric field on the growth orientation of CNTs. This finding contributes to a better understanding and engineering of the electric field-assisted growth of CNTs. Furthermore, the obtained statistical data are beneficial for the study of the polarization of CNTs in an electric field. There is currently a lack of experimental data in this research field.

This thesis has also provided interesting preliminary results for further studies. The results suggest that: (i) a rectifying CNT-Si contact could be converted into an ohmic contact after the local deposition of Pt at the CNT-Si contact; (ii) the reversibility of a NH_3 gas sensor using a Si/CNTs/Si system could be improved by switching off the bias voltage during the evacuation periods; and (iii) thermal evaporation of metals could be used to functionalize the suspended CNTs in the Si/CNTs/Si systems. However, the mechanism of the reversing process in the NH_3 sensor experiment has not yet been found, and the sensing performance of the functionalized CNTs has not yet been tested. There is thus a need for further studies.

Bibliography

[1] S. Iijima *et al.*, "Helical microtubules of graphitic carbon," *nature*, vol. 354, no. 6348, pp. 56–58, 1991.

[2] A. Krishnan, E. Dujardin, T. Ebbesen, P. Yianilos, and M. Treacy, "Young's modulus of single-walled nanotubes," *Physical Review B*, vol. 58, no. 20, p. 14013, 1998.

[3] M. Siegal, D. Overmyer, and P. Provencio, "Precise control of multiwall carbon nanotube diameters using thermal chemical vapor deposition," *Applied Physics Letters*, vol. 80, no. 12, pp. 2171–2173, 2002.

[4] X. Wang, Q. Li, J. Xie, Z. Jin, J. Wang, Y. Li, K. Jiang, and S. Fan, "Fabrication of ultralong and electrically uniform single-walled carbon nanotubes on clean substrates," *Nano Letters*, vol. 9, no. 9, pp. 3137–3141, 2009.

[5] B. Lukic, J. W. Seo, R. R. Bacsa, S. Delpeux, F. Béguin, G. Bister, A. Fonseca, J. B. Nagy, A. Kis, S. Jeney, *et al.*, "Catalytically grown carbon nanotubes of small diameter have a high young's modulus," *Nano Letters*, vol. 5, no. 10, pp. 2074–2077, 2005.

[6] B. Demczyk, Y. Wang, J. Cumings, M. Hetman, W. Han, A. Zettl, and R. Ritchie, "Direct mechanical measurement of the tensile strength and elastic modulus of multiwalled carbon nanotubes," *Materials Science and Engineering: A*, vol. 334, no. 1, pp. 173–178, 2002.

[7] J. P. Lu, "Elastic properties of carbon nanotubes and nanoropes," *Physical Review Letters*, vol. 79, no. 7, p. 1297, 1997.

[8] B. I. Yakobson and P. Avouris, "Mechanical properties of carbon nanotubes," in *Carbon Nanotubes*, pp. 287–327, Springer, 2001.

[9] P. Kim, L. Shi, A. Majumdar, and P. McEuen, "Thermal transport measurements of individual multiwalled nanotubes," *Physical Review Letters*, vol. 87, no. 21, p. 215502, 2001.

[10] S. Berber, Y.-K. Kwon, and D. Tomanek, "Unusually high thermal conductivity of carbon nanotubes," *Physical Review Letters*, vol. 84, no. 20, p. 4613, 2000.

[11] B. Wei, R. Vajtai, and P. Ajayan, "Reliability and current carrying capacity of carbon nanotubes," *Applied Physics Letters*, vol. 79, no. 8, pp. 1172–1174, 2001.

[12] S. Frank, P. Poncharal, Z. Wang, and W. A. de Heer, "Carbon nanotube quantum resistors," *Science*, vol. 280, no. 5370, pp. 1744–1746, 1998.

[13] Y. Wang and J. T. Yeow, "A review of carbon nanotubes-based gas sensors," *Journal of Sensors*, vol. 2009, 2009.

[14] P. G. Collins, K. Bradley, M. Ishigami, and A. Zettl, "Extreme oxygen sensitivity of electronic properties of carbon nanotubes," *Science*, vol. 287, no. 5459, pp. 1801–1804, 2000.

[15] R. H. Baughman, C. Cui, A. A. Zakhidov, Z. Iqbal, J. N. Barisci, G. M. Spinks, G. G. Wallace, A. Mazzoldi, D. De Rossi, A. G. Rinzler, *et al.*, "Carbon nanotube actuators," *Science*, vol. 284, no. 5418, pp. 1340–1344, 1999.

[16] K. Besteman, J.-O. Lee, F. G. Wiertz, H. A. Heering, and C. Dekker, "Enzyme-coated carbon nanotubes as single-molecule biosensors," *Nano Letters*, vol. 3, no. 6, pp. 727–730, 2003.

[17] A. Fennimore, T. Yuzvinsky, W.-Q. Han, M. Fuhrer, J. Cumings, and A. Zettl, "Rotational actuators based on carbon nanotubes," *Nature*, vol. 424, no. 6947, pp. 408–410, 2003.

[18] A. Modi, N. Koratkar, E. Lass, B. Wei, and P. M. Ajayan, "Miniaturized gas ionization sensors using carbon nanotubes," *Nature*, vol. 424, no. 6945, pp. 171–174, 2003.

[19] Y. Saito, K. Nishikubo, K. Kawabata, and T. Matsumoto, "Carbon nanocapsules and single-layered nanotubes produced with platinum-group metals (ru, rh, pd, os, ir, pt) by arc discharge," *Journal of Applied Physics*, vol. 80, no. 5, pp. 3062–3067, 1996.

[20] S. Farhat, M. L. de La Chapelle, A. Loiseau, C. D. Scott, S. Lefrant, C. Journet, and P. Bernier, "Diameter control of single-walled carbon nanotubes using argon–helium mixture gases," *The Journal of Chemical Physics*, vol. 115, p. 6752, 2001.

[21] D. Tang, S. Xie, W. Liu, B. Chang, L. Sun, Z. Liu, G. Wan, and W. Zhou, "Evidence for an open-ended nanotube growth model in arc discharge," *Carbon*, vol. 38, no. 3, pp. 480–483, 2000.

[22] T. Ebbesen and P. Ajayan, "Large-scale synthesis of carbon nanotubes," *Nature*, vol. 358, no. 6383, pp. 220–222, 1992.

[23] T. Guo, P. Nikolaev, A. Thess, D. Colbert, and R. Smalley, "Catalytic growth of single-walled manotubes by laser vaporization," *Chemical Physics Letters*, vol. 243, no. 1, pp. 49–54, 1995.

[24] N. Braidy, M. El Khakani, and G. Botton, "Effect of laser intensity on yield and physical characteristics of single wall carbon nanotubes produced by the nd: Yag laser vaporization method," *Carbon*, vol. 40, no. 15, pp. 2835–2842, 2002.

[25] A. Puretzky, D. Geohegan, X. Fan, and S. Pennycook, "Dynamics of single-wall carbon nanotube synthesis by laser vaporization," *Applied Physics A*, vol. 70, no. 2, pp. 153–160, 2000.

[26] C. D. Scott, S. Arepalli, P. Nikolaev, and R. E. Smalley, "Growth mechanisms for single-wall carbon nanotubes in a laser-ablation process," *Applied Physics A*, vol. 72, no. 5, pp. 573–580, 2001.

[27] A. Bolshakov, S. Uglov, A. Saveliev, V. Konov, A. Gorbunov, W. Pompe, and A. Graff, "A novel cw laser–powder method of carbon single-wall nanotubes production," *Diamond and Related Materials*, vol. 11, no. 3, pp. 927–930, 2002.

[28] F. Kokai, K. Takahashi, M. Yudasaka, R. Yamada, T. Ichihashi, and S. Iijima, "Growth dynamics of single-wall carbon nanotubes synthesized by co2 laser vaporization," *The Journal of Physical Chemistry B*, vol. 103, no. 21, pp. 4346–4351, 1999.

[29] M. Endo, K. Takeuchi, S. Igarashi, K. Kobori, M. Shiraishi, and H. W. Kroto, "The production and structure of pyrolytic carbon nanotubes (pcnts)," *Journal of Physics and Chemistry of Solids*, vol. 54, no. 12, pp. 1841–1848, 1993.

[30] C. J. Lee, D. W. Kim, T. J. Lee, Y. C. Choi, Y. S. Park, Y. H. Lee, W. B. Choi, N. S. Lee, G.-S. Park, and J. M. Kim, "Synthesis of aligned carbon nanotubes using thermal chemical vapor deposition," *Chemical Physics Letters*, vol. 312, no. 5, pp. 461–468, 1999.

[31] M. Meyyappan, L. Delzeit, A. Cassell, and D. Hash, "Carbon nanotube growth by pecvd: a review," *Plasma Sources Science and Technology*, vol. 12, no. 2, p. 205, 2003.

[32] A. Jungen, C. Stampfer, J. Hoetzel, V. M. Bright, and C. Hierold, "Process integration of carbon nanotubes into microelectromechanical systems," *Sensors and Actuators A: Physical*, vol. 130, pp. 588–594, 2006.

[33] A. Jungen, C. Stampfer, J. Hoetzel, and C. Hierold, "Novel process flow for the integration of carbon nanotubes into mems," in *Solid-State Sensors, Actuators and Microsystems, 2005. Digest of Technical Papers. TRANSDUCERS'05. The 13th International Conference on*, vol. 1, pp. 105–108, IEEE, 2005.

[34] C. Hierold, A. Jungen, C. Stampfer, and T. Helbling, "Nano electromechanical sensors based on carbon nanotubes," *Sensors and Actuators A: Physical*, vol. 136, no. 1, pp. 51–61, 2007.

[35] O. Englander, D. Christensen, and L. Lin, "Local synthesis of silicon nanowires and carbon nanotubes on microbridges," *Applied Physics Letters*, vol. 82, no. 26, pp. 4797–4799, 2003.

[36] O. Englander, D. Christensen, and L. Lin, "The integration of nanowires and nanotubes with microstructures," *International Journal of Materials and Product Technology*, vol. 34, no. 1, pp. 77–94, 2009.

[37] D. Christensen, O. Englander, J. Kim, and L. Lin, "Room temperature local synthesis of carbon nanotubes," in *Nanotechnology, 2003. IEEE-NANO 2003. 2003 Third IEEE Conference on*, vol. 2, pp. 581–584, IEEE, 2003.

[38] T. Kawano, D. Christensen, S. Chen, C. Y. Cho, and L. Lin, "Formation and characterization of silicon/carbon nanotube/silicon heterojunctions by local synthesis and assembly," *Applied Physics Letters*, vol. 89, no. 16, pp. 163510–163510, 2006.

[39] D. S. Engstrøm, N. L. Rupesinghe, K. B. Teo, W. I. Milne, and P. Bøgild, "Vertically aligned cnt growth on a microfabricated silicon heater with integrated temperature control-determination of the activation energy from a continuous thermal gradient," *Journal of Micromechanics and Microengineering*, vol. 21, no. 1, p. 015004, 2011.

[40] D.-Y. Kim, J. H. Choi, A. R. Zoulkarneev, M. H. Yang, I. T. Han, H. J. Kim, S. I. Kim, C. W. Baik, J.-H. Park, J.-B. Yoo, *et al.*, "Selective formation of carbon nanotubes and its application to field-emitter arrays," *Electron Device Letters, IEEE*, vol. 30, no. 7, pp. 709–711, 2009.

[41] Y. Zhou, J. L. Johnson, A. Ural, and H. Xie, "Localized growth of carbon nanotubes on cmos substrate at room temperature using maskless post-cmos processing," *Nanotechnology, IEEE Transactions on*, vol. 11, no. 1, pp. 16–20, 2012.

[42] S. Dittmer, O. Nerushev, and E. E. Campbell, "Low ambient temperature cvd growth of carbon nanotubes," *Applied Physics A*, vol. 84, no. 3, pp. 243–246, 2006.

[43] S. Dittmer, S. Mudgal, O. Nerushev, and E. E. Campbell, "Local heating method for growth of aligned carbon nanotubes at low ambient temperature," *Low Temperature Physics*, vol. 34, p. 834, 2008.

[44] S. Dittmer, J. Ek-Weis, O. Nerushev, and E. Campbell, "Growth of aligned mwnt arrays using a micrometer scale local-heater at low ambient temperature," *Journal of Nanoscience and Nanotechnology*, vol. 10, no. 6, pp. 4015–4022, 2010.

[45] Y. Zhou, J. Johnson, L. Wu, S. Maley, A. Ural, and H. Xie, "Design and fabrication of microheaters for localized carbon nanotube growth," in *Nanotechnology, 2008. NANO'08. 8th IEEE Conference on*, pp. 452–455, IEEE, 2008.

[46] W.-C. Lin, Y.-J. Yang, G.-W. Hsieh, C.-H. Tsai, C.-C. Chen, and C.-C. Liang, "Selective local synthesis of nanowires on a microreactor chip," *Sensors and Actuators A: Physical*, vol. 130, pp. 625–632, 2006.

[47] S. Bondi, W. Lackey, R. Johnson, X. Wang, and Z. Wang, "Laser assisted chemical vapor deposition synthesis of carbon nanotubes and their characterization," *Carbon*, vol. 44, no. 8, pp. 1393–1403, 2006.

[48] H. Abed, A. Charrier, H. Dallaporta, V. Safarov, H. Jamgotchian, and D. Tonneau, "Directed growth of horizontal silicon nanowires by laser induced decomposition of silane," *Journal of Vacuum Science & Technology B: Microelectronics and Nanometer Structures*, vol. 24, no. 3, pp. 1248–1253, 2006.

[49] J. Shi, Y. Lu, K. Yi, Y. Lin, S. Liou, J. Hou, and X. Wang, "Direct synthesis of single-walled carbon nanotubes bridging metal electrodes by laser-assisted chemical vapor deposition," *Applied Physics Letters*, vol. 89, no. 8, pp. 083105–083105, 2006.

[50] J. Park, S. Jeong, M. Jeong, S. Lim, I. Lee, and Y. Lee, "The rapid growth of vertically aligned carbon nanotubes using laser heating," *Nanotechnology*, vol. 20, no. 18, p. 185604, 2009.

[51] L. Cao, D. N. Barsic, A. R. Guichard, and M. L. Brongersma, "Plasmon-assisted local temperature control to pattern individual semiconductor nanowires and carbon nanotubes," *Nano Letters*, vol. 7, no. 11, pp. 3523–3527, 2007.

[52] D. A. Boyd, L. Greengard, M. Brongersma, M. Y. El-Naggar, and D. G. Goodwin, "Plasmon-assisted chemical vapor deposition," *Nano Letters*, vol. 6, no. 11, pp. 2592–2597, 2006.

[53] B. D. Sosnowchik and L. Lin, "Rapid synthesis of carbon nanotubes via inductive heating," *Applied Physics Letters*, vol. 89, no. 19, pp. –, 2006.

[54] T. Kawano, H. C. Chiamori, M. Suter, Q. Zhou, B. D. Sosnowchik, and L. Lin, "An electrothermal carbon nanotube gas sensor," *Nano Letters*, vol. 7, no. 12, pp. 3686–3690, 2007.

[55] H. Chiamori, X. Wu, X. Guo, B. Q. Ta, and L. Lin, "Annealing nano-to-micro contacts for improved contact resistance," in *Nano/Micro Engineered and Molecular Systems (NEMS), 2010 5th IEEE International Conference on*, pp. 666–670, IEEE, 2010.

[56] T. Kawano, M. Suter, C. Cho, H. Chiamori, and L. Lin, "Single carbon nanotube pirani gauge by local synthesis," in *Solid-State Sensors, Actuators and Microsystems Conference, 2007. TRANSDUCERS 2007. International*, pp. 1015–1018, IEEE, 2007.

[57] A. Jungen, C. Stampfer, M. Tonteling, S. Schiesser, D. Sarangi, and C. Hierold, "Localized and cmos compatible growth of carbon nanotubes on a 3× 3 μm< sup> 2</sup> microheater spot," in *Solid-State Sensors, Actuators and Microsystems, 2005. Digest of Technical Papers. TRANSDUCERS'05. The 13th International Conference on*, vol. 1, pp. 93–96, IEEE, 2005.

[58] L. Dong, A. Subramanian, D. Hugentobler, B. J. Nelson, and Y. Sun, "Nano encoders based on vertical arrays of individual carbon nanotubes," *Advanced Robotics*, vol. 20, no. 11, pp. 1281–1301, 2006.

[59] M. S. Dresselhaus, G. Dresselhaus, and P. C. Eklund, *Science of fullerenes and carbon nanotubes: their properties and applications*. Academic Press, 1996.

[60] J. W. Wilder, L. C. Venema, A. G. Rinzler, R. E. Smalley, and C. Dekker, "Electronic structure of atomically resolved carbon nanotubes," *Nature*, vol. 391, no. 6662, pp. 59–62, 1998.

[61] T. W. Odom, J.-L. Huang, P. Kim, and C. M. Lieber, "Atomic structure and electronic properties of single-walled carbon nanotubes," *Nature*, vol. 391, no. 6662, pp. 62–64, 1998.

[62] A. Bachtold, M. Fuhrer, S. Plyasunov, M. Forero, E. H. Anderson, A. Zettl, and P. L. McEuen, "Scanned probe microscopy of electronic transport in carbon nanotubes," *Physical Review Letters*, vol. 84, no. 26, p. 6082, 2000.

[63] S. Li, Z. Yu, C. Rutherglen, and P. J. Burke, "Electrical properties of 0.4 cm long single-walled carbon nanotubes," *Nano Letters*, vol. 4, no. 10, pp. 2003–2007, 2004.

[64] J. Mintmire, B. Dunlap, and C. White, "Are fullerene tubules metallic?," *Physical Review Letters*, vol. 68, no. 5, p. 631, 1992.

[65] R. Jishi, M. Dresselhaus, and G. Dresselhaus, "Electron-phonon coupling and the electrical conductivity of fullerene nanotubules," *Physical Review B*, vol. 48, no. 15, p. 11385, 1993.

[66] N. Hamada, S.-i. Sawada, and A. Oshiyama, "New one-dimensional conductors: Graphitic microtubules," *Physical Review Letters*, vol. 68, no. 10, p. 1579, 1992.

[67] K. Tanaka, K. Okahara, M. Okada, and T. Yamabe, "Electronic properties of bucky-tube model," *Chemical Physics Letters*, vol. 191, no. 5, pp. 469–472, 1992.

[68] C. White, D. Robertson, and J. Mintmire, "Helical and rotational symmetries of nanoscale graphitic tubules," *Physical Review B*, vol. 47, no. 9, p. 5485, 1993.

[69] R. Saito, M. Fujita, G. Dresselhaus, and M. Dresselhaus, "Electronic structure of chiral graphene tubules," *Applied Physics Letters*, vol. 60, p. 2204, 1992.

[70] V. Derycke, R. Martel, J. Appenzeller, and P. Avouris, "Carbon nanotube inter-and intramolecular logic gates," *Nano Letters*, vol. 1, no. 9, pp. 453–456, 2001.

[71] R. Martel, V. Derycke, J. Appenzeller, S. Wind, and P. Avouris, "Carbon nanotube field-effect transistors and logic circuits," in *Design Automation Conference, 2002. Proceedings. 39th*, pp. 94–98, IEEE, 2002.

[72] V. Derycke, R. Martel, J. Appenzeller, and P. Avouris, "Controlling doping and carrier injection in carbon nanotube transistors," *Applied Physics Letters*, vol. 80, p. 2773, 2002.

[73] M. Bockrath, J. Hone, A. Zettl, P. L. McEuen, A. G. Rinzler, and R. E. Smalley, "Chemical doping of individual semiconducting carbon-nanotube ropes," *Physical Review B*, vol. 61, no. 16, p. R10606, 2000.

[74] X. Yang, M. A. Guillorn, D. Austin, A. V. Melechko, H. Cui, H. M. Meyer, V. I. Merkulov, J. Caughman, D. H. Lowndes, and M. L. Simpson, "Fabrication and characterization of carbon nanofiber-based vertically integrated schottky barrier junction diodes," *Nano Letters*, vol. 3, no. 12, pp. 1751–1755, 2003.

[75] F. Kreupl, A. P. Graham, G. Duesberg, W. Steinhögl, M. Liebau, E. Unger, and W. Hönlein, "Carbon nanotubes in interconnect applications," *Microelectronic Engineering*, vol. 64, no. 1, pp. 399–408, 2002.

[76] Y. Chai, Z. Xiao, and P. C. Chan, "Low-resistance carbon nanotube contact plug to silicon," *Electron Device Letters, IEEE*, vol. 30, no. 8, pp. 811–813, 2009.

[77] S. S. Li, *Semiconductor physical electronics*. Springer Berlin, 2006.

[78] H. Ago, T. Kugler, F. Cacialli, W. R. Salaneck, M. S. Shaffer, A. H. Windle, and R. H. Friend, "Work functions and surface functional groups of multiwall carbon nanotubes," *The Journal of Physical Chemistry B*, vol. 103, no. 38, pp. 8116–8121, 1999.

[79] "Physical properties of semiconductors @ONLINE." Date: Jan. 6th 2010. URL: http://www.ioffe.ru/SVA/NSM/.

[80] S. M. Sze and K. K. Ng, *Physics of semiconductor devices*. Wiley. com, 2006.

[81] K. K. Ng and R. Liu, "On the calculation of specific contact resistivity on< 100> si," *Electron Devices, IEEE Transactions on*, vol. 37, no. 6, pp. 1535–1537, 1990.

[82] Z. Chen, J. Appenzeller, J. Knoch, Y.-m. Lin, and P. Avouris, "The role of metal-nanotube contact in the performance of carbon nanotube field-effect transistors," *Nano Letters*, vol. 5, no. 7, pp. 1497–1502, 2005.

[83] M. Liebau, E. Unger, G. Duesberg, A. Graham, R. Seidel, F. Kreupl, and W. Hoenlein, "Contact improvement of carbon nanotubes via electroless nickel deposition," *Applied Physics A*, vol. 77, no. 6, pp. 731–734, 2003.

[84] S. Heinze, J. Tersoff, R. Martel, V. Derycke, J. Appenzeller, and P. Avouris, "Carbon nanotubes as schottky barrier transistors," *Physical Review Letters*, vol. 89, no. 10, p. 106801, 2002.

[85] J. Kong, C. Zhou, A. Morpurgo, H. Soh, C. Quate, C. Marcus, and H. Dai, "Synthesis, integration, and electrical properties of individual single-walled carbon nanotubes," *Applied Physics A*, vol. 69, no. 3, pp. 305–308, 1999.

[86] X.-P. Tang, A. Kleinhammes, H. Shimoda, L. Fleming, K. Bennoune, S. Sinha, C. Bower, O. Zhou, and Y. Wu, "Electronic structures of single-walled carbon nanotubes determined by nmr," *Science*, vol. 288, no. 5465, pp. 492–494, 2000.

[87] G. Sumanasekera, C. Adu, S. Fang, and P. Eklund, "Effects of gas adsorption and collisions on electrical transport in single-walled carbon nanotubes," *Physical Review Letters*, vol. 85, no. 5, p. 1096, 2000.

[88] J. Kong, M. G. Chapline, and H. Dai, "Functionalized carbon nanotubes for molecular hydrogen sensors," *Advanced Materials*, vol. 13, no. 18, pp. 1384–1386, 2001.

[89] F. Picaud, R. Langlet, M. Arab, M. Devel, C. Girardet, S. Natarajan, S. Chopra, and A. Rao, "Gas-induced variation in the dielectric properties of carbon nanotube bundles for selective sensing," *Journal of Applied Physics*, vol. 97, no. 11, pp. 114316–114316, 2005.

[90] S. Chopra, K. McGuire, N. Gothard, A. Rao, and A. Pham, "Selective gas detection using a carbon nanotube sensor," *Applied Physics Letters*, vol. 83, no. 11, pp. 2280–2282, 2003.

[91] O. Varghese, P. Kichambre, D. Gong, K. Ong, E. Dickey, and C. Grimes, "Gas sensing characteristics of multi-wall carbon nanotubes," *Sensors and Actuators B: Chemical*, vol. 81, no. 1, pp. 32–41, 2001.

[92] K. G. Ong, K. Zeng, and C. A. Grimes, "A wireless, passive carbon nanotube-based gas sensor," *Sensors Journal, IEEE*, vol. 2, no. 2, pp. 82–88, 2002.

[93] R. Roy, M. P. Chowdhury, and A. Pal, "Room temperature sensor based on carbon nanotubes and nanofibres for methane detection," *Vacuum*, vol. 77, no. 3, pp. 223–229, 2005.

[94] E. Snow, F. Perkins, E. Houser, S. Badescu, and T. Reinecke, "Chemical detection with a single-walled carbon nanotube capacitor," *Science*, vol. 307, no. 5717, pp. 1942–1945, 2005.

[95] M. Penza, F. Antolini, and M. V. Antisari, "Carbon nanotubes as saw chemical sensors materials," *Sensors and Actuators B: Chemical*, vol. 100, no. 1, pp. 47–59, 2004.

[96] T. Someya, J. Small, P. Kim, C. Nuckolls, and J. T. Yardley, "Alcohol vapor sensors based on single-walled carbon nanotube field effect transistors," *Nano Letters*, vol. 3, no. 7, pp. 877–881, 2003.

[97] J. Wang and M. Musameh, "Carbon nanotube/teflon composite electrochemical sensors and biosensors," *Analytical chemistry*, vol. 75, no. 9, pp. 2075–2079, 2003.

[98] Y. Liang, Y. Chen, and T. Wang, "Low-resistance gas sensors fabricated from multi-walled carbon nanotubes coated with a thin tin oxide layer," *Applied Physics Letters*, vol. 85, no. 4, pp. 666–668, 2004.

[99] C. Staii, A. T. Johnson, M. Chen, and A. Gelperin, "Dna-decorated carbon nanotubes for chemical sensing," *Nano Letters*, vol. 5, no. 9, pp. 1774–1778, 2005.

[100] J. Suehiro, G. Zhou, H. Imakiire, W. Ding, and M. Hara, "Controlled fabrication of carbon nanotube no< sub> 2</sub> gas sensor using dielectrophoretic impedance measurement," *Sensors and Actuators B: Chemical*, vol. 108, no. 1, pp. 398–403, 2005.

[101] J. Li, Y. Lu, Q. Ye, M. Cinke, J. Han, and M. Meyyappan, "Carbon nanotube sensors for gas and organic vapor detection," *Nano Letters*, vol. 3, no. 7, pp. 929–933, 2003.

[102] B. Matthews, J. Li, S. Sunshine, L. Lerner, and J. W. Judy, "Effects of electrode configuration on polymer carbon-black composite chemical vapor sensor performance," *Sensors Journal, IEEE*, vol. 2, no. 3, pp. 160–168, 2002.

[103] T. K. Starke and G. S. Coles, "High sensitivity ozone sensors for environmental monitoring produced using laser ablated nanocrystalline metal oxides," *Sensors Journal, IEEE*, vol. 2, no. 1, pp. 14–19, 2002.

[104] L. Valentini, F. Mercuri, I. Armentano, C. Cantalini, S. Picozzi, L. Lozzi, S. Santucci, A. Sgamellotti, and J. Kenny, "Role of defects on the gas sensing properties of carbon nanotubes thin films: experiment and theory," *Chemical Physics Letters*, vol. 387, no. 4, pp. 356–361, 2004.

[105] J. A. Robinson, E. S. Snow, S. C. Badescu, T. L. Reinecke, and F. K. Perkins, "Role of defects in single-walled carbon nanotube chemical sensors," *Nano Letters*, vol. 6, no. 8, pp. 1747–1751, 2006.

[106] P. C. Watts, N. Mureau, Z. Tang, Y. Miyajima, J. D. Carey, and S. R. P. Silva, "The importance of oxygen-containing defects on carbon nanotubes for the detection of polar and non-polar vapours through hydrogen bond formation," *Nanotechnology*, vol. 18, no. 17, p. 175701, 2007.

[107] D. Fu, H. Lim, Y. Shi, X. Dong, S. Mhaisalkar, Y. Chen, S. Moochhala, and L.-J. Li, "Differentiation of gas molecules using flexible and all-carbon nanotube devices," *The Journal of Physical Chemistry C*, vol. 112, no. 3, pp. 650–653, 2008.

[108] J. Chen, M. A. Hamon, H. Hu, Y. Chen, A. M. Rao, P. C. Eklund, and R. C. Haddon, "Solution properties of single-walled carbon nanotubes," *Science*, vol. 282, no. 5386, pp. 95–98, 1998.

[109] M. Hamon, H. Hu, P. Bhowmik, S. Niyogi, B. Zhao, M. Itkis, and R. Haddon, "End-group and defect analysis of soluble single-walled carbon nanotubes," *Chemical Physics Letters*, vol. 347, no. 1, pp. 8–12, 2001.

[110] A. Star, J. F. Stoddart, D. Steuerman, M. Diehl, A. Boukai, E. W. Wong, X. Yang, S.-W. Chung, H. Choi, and J. R. Heath, "Preparation and properties of polymer-wrapped single-walled carbon nanotubes," *Angewandte Chemie International Edition*, vol. 40, no. 9, pp. 1721–1725, 2001.

[111] H. Xia, Q. Wang, and G. Qiu, "Polymer-encapsulated carbon nanotubes prepared through ultrasonically initiated in situ emulsion polymerization," *Chemistry of materials*, vol. 15, no. 20, pp. 3879–3886, 2003.

[112] M. K. Kumar and S. Ramaprabhu, "Nanostructured pt functionlized multiwalled carbon nanotube based hydrogen sensor," *The Journal of Physical Chemistry B*, vol. 110, no. 23, pp. 11291–11298, 2006.

[113] Y. Lu, J. Li, J. Han, H.-T. Ng, C. Binder, C. Partridge, and M. Meyyappan, "Room temperature methane detection using palladium loaded single-walled carbon nanotube sensors," *Chemical Physics Letters*, vol. 391, no. 4, pp. 344–348, 2004.

[114] I. Sayago, E. Terrado, M. Aleixandre, M. Horrillo, M. Fernández, J. Lozano, E. Lafuente, W. Maser, A. Benito, M. Martinez, *et al.*, "Novel selective sensors based on carbon nanotube films for hydrogen detection," *Sensors and Actuators B: Chemical*, vol. 122, no. 1, pp. 75–80, 2007.

[115] S. Mubeen, T. Zhang, B. Yoo, M. A. Deshusses, and N. V. Myung, "Palladium nanoparticles decorated single-walled carbon nanotube hydrogen sensor," *The Journal of Physical Chemistry C*, vol. 111, no. 17, pp. 6321–6327, 2007.

[116] P. Young, Y. Lu, R. Terrill, and J. Li, "High-sensitivity no2 detection with carbon nanotube-gold nanoparticle composite films," *Journal of Nanoscience and Nanotechnology*, vol. 5, no. 9, pp. 1509–1513, 2005.

[117] M. Penza, R. Rossi, M. Alvisi, G. Cassano, M. Signore, E. Serra, and R. Giorgi, "Pt- and pd-nanoclusters functionalized carbon nanotubes networked films for sub-ppm gas sensors," *Sensors and Actuators B: Chemical*, vol. 135, no. 1, pp. 289–297, 2008.

[118] M. Penza, G. Cassano, R. Rossi, M. Alvisi, A. Rizzo, M. Signore, T. Dikonimos, E. Serra, and R. Giorgi, "Enhancement of sensitivity in gas chemiresistors based on carbon nanotube surface functionalized with noble metal (au, pt) nanoclusters," *Applied Physics Letters*, vol. 90, no. 17, pp. 173123–173123, 2007.

[119] A. Star, V. Joshi, S. Skarupo, D. Thomas, and J.-C. P. Gabriel, "Gas sensor array based on metal-decorated carbon nanotubes," *The Journal of Physical Chemistry B*, vol. 110, no. 42, pp. 21014–21020, 2006.

[120] Y. Lu, C. Partridge, M. Meyyappan, and J. Li, "A carbon nanotube sensor array for sensitive gas discrimination using principal component analysis," *Journal of Electroanalytical Chemistry*, vol. 593, no. 1, pp. 105–110, 2006.

[121] M. Cadek, R. Murphy, B. McCarthy, A. Drury, B. Lahr, R. Barklie, J. Coleman, W. Blau, *et al.*, "Optimisation of the arc-discharge production of multi-walled carbon nanotubes," *Carbon*, vol. 40, no. 6, pp. 923–928, 2002.

[122] S.-H. Jung, M.-R. Kim, S.-H. Jeong, S.-U. Kim, O.-J. Lee, K.-H. Lee, J.-H. Suh, and C.-K. Park, "High-yield synthesis of multi-walled carbon nanotubes by arc discharge in liquid nitrogen," *Applied Physics A*, vol. 76, no. 2, pp. 285–286, 2003.

[123] C.-H. Kiang, W. A. Goddard, R. Beyers, and D. S. Bethune, "Carbon nanotubes with single-layer walls," *Carbon*, vol. 33, no. 7, pp. 903–914, 1995.

[124] C. Journet and P. Bernier, "Production of carbon nanotubes," *Applied Physics A: Materials Science & Processing*, vol. 67, no. 1, pp. 1–9, 1998.

[125] M. Yudasaka, F. Kokai, K. Takahashi, R. Yamada, N. Sensui, T. Ichihashi, and S. Iijima, "Formation of single-wall carbon nanotubes: Comparison of co2 laser ablation and nd: Yag laser ablation," *The Journal of Physical Chemistry B*, vol. 103, no. 18, pp. 3576–3581, 1999.

[126] P. Eklund, B. Pradhan, U. Kim, Q. Xiong, J. Fischer, A. Friedman, B. Holloway, K. Jordan, and M. Smith, "Large-scale production of single-walled carbon nanotubes using ultrafast pulses from a free electron laser," *Nano Letters*, vol. 2, no. 6, pp. 561–566, 2002.

[127] K. Hirahara, K. Suenaga, S. Bandow, and S. Iijima, "Boron-catalyzed multi-walled carbon nanotube growth with the reduced number of layers by laser ablation," *Chemical Physics Letters*, vol. 324, no. 1, pp. 224–230, 2000.

[128] M. Yudasaka, T. Ichihashi, and S. Iijima, "Roles of laser light and heat in formation of single-wall carbon nanotubes by pulsed laser ablation of cxniycoy targets at high temperature," *The Journal of Physical Chemistry B*, vol. 102, no. 50, pp. 10201–10207, 1998.

[129] W. Maser, E. Munoz, A. Benito, M. Martınez, G. De La Fuente, Y. Maniette, E. Anglaret, and J.-L. Sauvajol, "Production of high-density single-walled nanotube material by a simple laser-ablation method," *Chemical Physics Letters*, vol. 292, no. 4, pp. 587–593, 1998.

[130] A. Rinzler, J. Liu, H. Dai, P. Nikolaev, C. Huffman, F. Rodriguez-Macias, P. Boul, A. H. Lu, D. Heymann, D. Colbert, *et al.*, "Large-scale purification of single-wall carbon nanotubes: process, product, and characterization," *Applied Physics A: Materials Science & Processing*, vol. 67, no. 1, pp. 29–37, 1998.

[131] R. Baker, M. Barber, P. Harris, F. Feates, and R. Waite, "Nucleation and growth of carbon deposits from the nickel catalyzed decomposition of acetylene," *Journal of Catalysis*, vol. 26, no. 1, pp. 51–62, 1972.

[132] R. Smajda, J. Andresen, M. Duchamp, R. Meunier, S. Casimirius, K. Hernadi, L. Forró, and A. Magrez, "Synthesis and mechanical properties of carbon nanotubes produced by the water assisted cvd process," *Physica Status Solidi (B)*, vol. 246, no. 11-12, pp. 2457–2460, 2009.

[133] S. Patole, P. Alegaonkar, H.-C. Lee, and J.-B. Yoo, "Optimization of water assisted chemical vapor deposition parameters for super growth of carbon nanotubes," *Carbon*, vol. 46, no. 14, pp. 1987–1993, 2008.

[134] H. R. Byon, H. Lim, H. J. Song, and H. C. Choi, "A synthesis of high purity single-walled carbon nanotubes from small diameters of cobalt nanoparticles by using oxygen-assisted chemical vapor deposition process," *Bulletin-Korean Chemical Society*, vol. 28, no. 11, p. 2056, 2007.

[135] D. Varshney, B. R. Weiner, and G. Morell, "Growth and field emission study of a monolithic carbon nanotube/diamond composite," *Carbon*, vol. 48, no. 12, pp. 3353–3358, 2010.

[136] K. Hee Dong, L. Jae-Hyeoung, and C. Won Seok, "Direct growth of carbon nanotubes with a catalyst of nickel nanoparticle-coated alumina powders," *Journal of Korean Physical Society*, vol. 58, p. 112, 2011.

[137] B. Brown, C. B. Parker, B. R. Stoner, and J. T. Glass, "Growth of vertically aligned bamboo-like carbon nanotubes from ammonia/methane precursors using a platinum catalyst," *Carbon*, vol. 49, no. 1, pp. 266–274, 2011.

[138] Y. Xu, E. Dervishi, A. R. Biris, and A. S. Biris, "Chirality-enriched semiconducting carbon nanotubes synthesized on high surface area mgo-supported catalyst," *Materials Letters*, vol. 65, no. 12, pp. 1878–1881, 2011.

[139] H. Zhu, C. Xu, D. Wu, B. Wei, R. Vajtai, and P. Ajayan, "Direct synthesis of long single-walled carbon nanotube strands," *Science*, vol. 296, no. 5569, pp. 884–886, 2002.

[140] S. Sato, A. Kawabata, M. Nihei, and Y. Awano, "Growth of diameter-controlled carbon nanotubes using monodisperse nickel nanoparticles obtained with a differential mobility analyzer," *Chemical Physics Letters*, vol. 382, no. 3, pp. 361–366, 2003.

[141] Z. Ren, Z. Huang, J. Xu, D. Wang, J. Wang, L. Calvet, J. Chen, J. Klemic, and M. Reed, "Large arrays of well-aligned carbon nanotubes," in *AIP Conference Proceedings*, vol. 486, p. 263, 1999.

[142] Z. Y. Juang, J. Lai, C. Weng, J. Lee, H. Lai, T. Lai, and C. Tsai, "On the kinetics of carbon nanotube growth by thermal cvd method," *Diamond and related materials*, vol. 13, no. 11, pp. 2140–2146, 2004.

[143] Z. Yu, S. Li, and P. J. Burke, "Synthesis of aligned arrays of millimeter long, straight single-walled carbon nanotubes," *Chemistry of Materials*, vol. 16, no. 18, pp. 3414–3416, 2004.

[144] R. Sen, A. Govindaraj, and C. Rao, "Carbon nanotubes by the metallocene route," *Chemical Physics Letters*, vol. 267, no. 3, pp. 276–280, 1997.

[145] M. Yudasaka, R. Kikuchi, Y. Ohki, E. Ota, and S. Yoshimura, "Behavior of ni in carbon nanotube nucleation," *Applied Physics Letters*, vol. 70, no. 14, pp. 1817–1818, 1997.

[146] T. Yamada, T. Namai, K. Hata, D. N. Futaba, K. Mizuno, J. Fan, M. Yudasaka, M. Yumura, and S. Iijima, "Size-selective growth of double-walled carbon nanotube forests from engineered iron catalysts," *Nature Nanotechnology*, vol. 1, no. 2, pp. 131–136, 2006.

[147] Y.-Q. Xu, E. Flor, M. J. Kim, B. Hamadani, H. Schmidt, R. E. Smalley, and R. H. Hauge, "Vertical array growth of small diameter single-walled carbon nanotubes," *Journal of the American Chemical Society*, vol. 128, no. 20, pp. 6560–6561, 2006.

[148] D. C. Meier, S. Semancik, B. Button, E. Strelcov, and A. Kolmakov, "Coupling nanowire chemiresistors with mems microhotplate gas sensing platforms," *Applied Physics Letters*, vol. 91, no. 6, pp. –, 2007.

[149] D. Whang, S. Jin, and C. M. Lieber, "Large-scale hierarchical organization of nanowires for functional nanosystems," *Japanese Journal of Applied Physics*, vol. 43, no. 7B, pp. 4465–4470, 2004.

[150] F. Patolsky, G. Zheng, and C. M. Lieber, "Fabrication of silicon nanowire devices for ultrasensitive, label-free, real-time detection of biological and chemical species," *Nature Protocols*, vol. 1, no. 4, pp. 1711–1724, 2006.

[151] R. He, D. Gao, R. Fan, A. Hochbaum, C. Carraro, R. Maboudian, and P. Yang, "Si nanowire bridges in microtrenches: Integration of growth into device fabrication," *Advanced Materials*, vol. 17, no. 17, pp. 2098–2102, 2005.

[152] L. Luo, B. D. Sosnowchik, and L. Lin, "Room temperature fast synthesis of zinc oxide nanowires by inductive heating," *Applied Physics Letters*, vol. 90, no. 9, pp. –, 2007.

[153] J. B. Park, S. H. Jeong, M. S. Jeong, S. C. Lim, I. H. Lee, and Y. H. Lee, "The rapid growth of vertically aligned carbon nanotubes using laser heating," *Nanotechnology*, vol. 20, no. 18, p. 185604, 2009.

[154] D. Koester, A. Cowen, R. Mahadevan, M. Stonefield, and B. Hardy, "Polymumps design handbook," *MEMSCAP Inc*, 2003.

[155] K. Miller, A. Cowen, G. Hames, and B. Hardy, "Soimumps design handbook," *MEMScAP Inc., Durham*, 2004.

[156] T. B. Haugen, "Synthesis and characterization of locally grown carbon nanotubes," Master's thesis, Vestfold University College (HiVe).

[157] E. Joselevich and C. M. Lieber, "Vectorial growth of metallic and semiconducting single-wall carbon nanotubes," *Nano Letters*, vol. 2, no. 10, pp. 1137–1141, 2002.

[158] Y. Zhang, A. Chang, J. Cao, Q. Wang, W. Kim, Y. Li, N. Morris, E. Yenilmez, J. Kong, and H. Dai, "Electric-field-directed growth of aligned single-walled carbon nanotubes," *Applied Physics Letters*, vol. 79, no. 19, pp. 3155–3157, 2001.

[159] A. Ural, Y. Li, and H. Dai, "Electric-field-aligned growth of single-walled carbon nanotubes on surfaces," *Applied Physics Letters*, vol. 81, no. 18, pp. 3464–3466, 2002.

[160] S. Dittmer, J. Svensson, and E. Campbell, "Electric field aligned growth of single-walled carbon nanotubes," *Current Applied Physics*, vol. 4, no. 6, pp. 595 – 598, 2004.

[161] L. Huang, Z. Jia, and S. O'Brien, "Orientated assembly of single-walled carbon nanotubes and applications," *Journal of Materials Chemistry*, vol. 17, no. 37, pp. 3863–3874, 2007.

[162] T. B. Haugen, B. Q. Ta, E. Halvorsen, N. Hoivik, and K. E. Aasmundtveit, "Integration of carbon nanotubes in microsystems: Local growth and electrical properties of contacts," *Materials*, vol. 6, no. 8, pp. 3094–3107, 2013.

[163] J. Zhang, A. Boyd, A. Tselev, M. Paranjape, and P. Barbara, "Mechanism of no2 detection in carbon nanotube field effect transistor chemical sensors," *Applied Physics Letters*, vol. 88, p. 123112, 2006.

[164] N. Peng, Q. Zhang, C. L. Chow, O. K. Tan, and N. Marzari, "Sensing mechanisms for carbon nanotube based nh3 gas detection," *Nano Letters*, vol. 9, no. 4, pp. 1626–1630, 2009.

[165] E. Espinosa, R. Ionescu, C. Bittencourt, A. Felten, R. Erni, G. Van Tendeloo, J.-J. Pireaux, and E. Llobet, "Metal-decorated multi-wall carbon nanotubes for low temperature gas sensing," *Thin Solid Films*, vol. 515, no. 23, pp. 8322–8327, 2007.

[166] S. Ju, J. M. Lee, Y. Jung, E. Lee, W. Lee, and S.-J. Kim, "Highly sensitive hydrogen gas sensors using single-walled carbon nanotubes grafted with pd nanoparticles," *Sensors and Actuators B: Chemical*, vol. 146, no. 1, pp. 122–128, 2010.

[167] Y. Zhang and H. Dai, "Formation of metal nanowires on suspended single-walled carbon nanotubes," *Applied Physics Letters*, vol. 77, no. 19, pp. 3015–3017, 2000.

[168] A. V. Ngo, "Functionalization of carbon nanotubes by thermal evaporation and atomic layer deposition," Master's thesis, Vestfold University College (HiVe).

Publications

Papers are not available in this file due to publiser’s restrictions.